Supporting Information for

A Homologous Series of Co, Rh, and Ir Metalloradicals

Ayumi Takaoka, and Jonas C. Peters

Figure 1. ^{1}H NMR spectrum of {[SiP$^{i\mathrm{Pr}}_3$]Co(PMe$_3$)}BAr$^F_4$ (1).
Figure 2. NMR spectra of [SiP$^{i\mathrm{Pr}}_3$]Rh(H)(Cl) (7).
Figure 3. NMR spectra of [SiP$^{i\mathrm{Pr}}_3$]Rh(N$_2$) (5).
Figure 4. NMR spectra of [SiP$^{i\mathrm{Pr}}_3$]Rh(PMe$_3$) (8).
Figure 5. ^{1}H NMR spectrum of {[SiP$^{i\mathrm{Pr}}_3$]Rh(PMe$_3$)}BAr$^F_4$ (2).
Figure 6. NMR spectra of [SiP$^{i\mathrm{Pr}}_3$]Ir(PMe$_3$) (9).
Figure 7. ^{1}H NMR spectrum of {[SiP$^{i\mathrm{Pr}}_3$]Ir(PMe$_3$)}BAr$^F_4$ (3).
Figure 8. Cyclic Voltammogram of {[SiP$^{i\mathrm{Pr}}_3$]Co(PMe$_3$)}BAr$^F_4$ (1).
Figure 9. Cyclic Voltammogram of [SiP$^{i\mathrm{Pr}}_3$]Rh(PMe$_3$) (8).
Figure 10. Cyclic Voltammogram of [SiP$^{i\mathrm{Pr}}_3$]Ir(PMe$_3$) (8).
Figure 11. 77 K EPR spectrum of {[SiP$^{i\mathrm{Pr}}_3$]Co(PMe$_3$)}BAr$^F_4$ (1).
Figure 12. RT EPR spectrum of {[SiP$^{i\mathrm{Pr}}_3$]Rh(PMe$_3$)}BAr$^F_4$ (2).
Figure 13. 77 K EPR spectrum of {[SiP$^{i\mathrm{Pr}}_3$]Rh(PMe$_3$)}BAr$^F_4$ (2).
Figure 14. RT EPR spectrum of {[SiP$^{i\mathrm{Pr}}_3$]Ir(PMe$_3$)}BAr$^F_4$ (3).
Figure 15. 77 K EPR spectrum of {[SiP$^{i\mathrm{Pr}}_3$]Ir(PMe$_3$)}BAr$^F_4$ (3).
Table 1. Crystal data and structure refinement for {[SiP$^{i\mathrm{Pr}}_3$]Co(PMe$_3$)}BAr$^F_4$ (1)
Figure 16. Solid-state Structure of {[SiP$^{i\mathrm{Pr}}_3$]Co(PMe$_3$)}BAr$^F_4$ (1).
Table 2. Crystal data and structure refinement for {[SiP$^{i\mathrm{Pr}}_3$]Rh(PMe$_3$)}BAr$^F_4$ (2)
Figure 17. Solid-state Structure of {[SiP$^{i\mathrm{Pr}}_3$]Rh(PMe$_3$)}BAr$^F_4$ (2).
Table 3. Crystal data and structure refinement for {[SiP$^{i\mathrm{Pr}}_3$]Ir(PMe$_3$)}OTf (3')
Figure 18. Solid-state Structure of {[SiP$^{i\mathrm{Pr}}_3$]Ir(PMe$_3$)}OTf (3').
Table 4. Spin density calculated from optimized structure and x-ray coordinates of [SiP$^{i\mathrm{Pr}}_3$]Co(PMe$_3$)}BAr$^F_4$ (1).
Table 5. Coordinates of optimized structure of [SiP$^{i\mathrm{Pr}}_3$]Co(PMe$_3$)}BAr$^F_4$ (1).
Table 6. Coordinates of optimized structure of [SiP$^{i\mathrm{Pr}}_3$]Rh(PMe$_3$)}BAr$^F_4$ (2).
Table 7. Coordinates of optimized structure of [SiP$^{i\mathrm{Pr}}_3$]Ir(PMe$_3$)}BAr$^F_4$ (3).
Figure 19. UV-VIS spectrum of [SiP$^{i\mathrm{Pr}}_3$]Rh(N$_2$) (5) under N$_2$ and after several freeze-pump-thaw cycles.
Figure 20. Relative energies of the frontier orbitals for complexes 1-3 and their molecular orbitals.

General Considerations. All manipulations were carried out using standard Schlenk or glovebox techniques under an atmosphere of dinitrogen. Unless otherwise noted, solvents were degassed and dried by thoroughly sparging with N_2 gas followed by passage through an activated alumina column. Hexamethyldisiloxane was dried over CaH_2 and distilled. Pentane, hexamethyldisiloxane, benzene, methylcyclohexane, toluene, tetrahydrofuran, and diethylether were tested with a standard purple solution of sodium benzophenone ketyl in tetrahydrofuran. Unless noted otherwise, all reagents were purchased from commercial vendors and used without further purification. Celite (Celite® 545) was dried at 150 °C overnight before use. $FcBAr^F_4$,[1] $[SiP^{iPr}_3]Co(N_2)$, [2] and $[SiP^{iPr}_3]Ir(N_2)$[2] were prepared according to literature procedures. Deuterated solvents were purchased from Cambridge Isotope Laboratories, Inc., degassed, and stored over 3-Å molecular sieves prior to use. Elemental analyses were performed by Midwest Microlabs.

X-ray Crystallography Procedures. X-ray diffraction studies were carried out at the Beckman Institute Crystallography Facility on a Brüker KAPPA APEX II diffractometer and at the MIT Department of Chemistry X-Ray Diffraction Facility on a Bruker three-circle Platform APEX II diffractometer solved using SHELX v. 6.14. The crystals were mounted on a glass fiber with Paratone-N oil. Data were collected at 100 K using Mo Kα (λ = 0.710 73 Å) radiation and solved using SHELXS[3] and refined against F^2 on all data by full-matrix least squares with SHELXL.[3] X-ray quality crystals were grown as described in the experimental procedures.

Electrochemistry

Electrochemical measurements were carried out in a glovebox under a dinitrogen atmosphere in a one-compartment cell using a CH Instruments 600B electrochemical analyzer. A glassy carbon electrode was used as the working electrode and platinum wire was used as the auxillary electrode. The reference electrode was Ag/AgNO3 in THF. The ferrocene couple Fc+/Fc was

---

[1] J. Le Bras, H. Jiao, W. E. Meyer, F. Hampel, J. A. Gladysz, *J. Organomet. Chem.* **2000**, *616*, 54.

[2] M. T. Whited, N. P. Mankad, Y. Lee, P. F. Oblad, J. C. Peters, *Inorg. Chem.* **2009**, *48*, 2507

[3] Sheldrick, G. M. *Acta. Cryst.* **2008**, *A64*, 112.

used as an external reference. Solutions (THF) of electrolyte (0.3 M tetra-*n*-butylammonium hexafluorophosphate) and analyte were also prepared under an inert atmosphere.

DFT Calculations. Geometry optimization for **1**, **2**, and **3** were run on the Gaussian03[4] suite of programs with the B3LYP[5] level of theory with the LANL2TZ(f)[6] basis set for Co, Rh and Ir, 6-31G(d)[7] basis set for Si and P, and LANL2DZ[8] basis set for C and H atoms. Frequency calculations on **2** and **3** confirmed the optimized structures to be minima. For complex **1**, frequency calculations on the optimized structure yielded one imaginary frequency that involved a vibrational mode that depicts a slight rocking motion about the molecule. Using a pruned (99,590) grid instead of the default pruned (75302) grid also resulted in the same transition state.

---

[4] Gaussian 03, Revision C.02, M. J. Frisch, G. W. Trucks, H. B. Schlegel, G. E. Scuseria, M. A. Robb, J. R. Cheeseman, J. A. Montgomery, Jr., T. Vreven, K. N. Kudin, J. C. Burant, J. M. Millam, S. S. Iyengar, J. Tomasi, V. Barone, B. Mennucci, M. Cossi, G. Scalmani, N. Rega, G. A. Petersson, H. Nakatsuji, M. Hada, M. Ehara, K. Toyota, R. Fukuda, J. Hasegawa, M. Ishida, T. Nakajima, Y. Honda, O. Kitao, H. Nakai, M. Klene, X. Li, J. E. Knox, H. P. Hratchian, J. B. Cross, V. Bakken, C. Adamo, J. Jaramillo, R. Gomperts, R. E. Stratmann, O. Yazyev, A. J. Austin, R. Cammi, C. Pomelli, J. W. Ochterski, P. Y. Ayala, K. Morokuma, G. A. Voth, P. Salvador, J. J. Dannenberg, V. G. Zakrzewski, S. Dapprich, A. D. Daniels, M. C. Strain, O. Farkas, D. K. Malick, A. D. Rabuck, K. Raghavachari, J. B. Foresman, J. V. Ortiz, Q. Cui, A. G. Baboul, S. Clifford, J. Cioslowski, B. B. Stefanov, G. Liu, A. Liashenko, P. Piskorz, I. Komaromi, R. L. Martin, D. J. Fox, T. Keith, M. A. Al-Laham, C. Y. Peng, A. Nanayakkara, M. Challacombe, P. M. W. Gill, B. Johnson, W. Chen, M. W. Wong, C. Gonzalez, and J. A. Pople, Gaussian, Inc., Wallingford CT, 2004.

[5] a) Becke, A.D. *J. Chem. Phys.* **1993**, *98*, 5648. b) Lee, C.; Yang, W.; Parr, R. G. *Phys. Rev. B.* **1988**, *37*, 785.

[6] b) Hay, P. J.; Wadt, W. R. *J. Chem. Phys.* **1985**, *82*, 299. b) Roy, L. E.; Hay, P. J.; Martin, R. L. *J. Chem. Theory Comput.* **2008**, *4*, 1029. c) Ehlers, A. W.; Bohme, M.; Dapprich, S.; Gobbi, A.; Hollwarth, A.; Jonas, V.; Kohler, K. F.; Stegmann, R.; Veldkamp, A.; Frenking, G. *Chem. Phys. Lett.* **1993**, *208*, 111.

[7] a) Hariharan, P. C.; Pople, J. A. *Theoret. Chimica Acta.* **1973**, *28*, 213. b) Francl, M. M.; Petero, W. J.; Hehre, W. J.; Binkley, J. S.; Gordon, M. S.; DeFrees, D. J.; Pople, J. A. *J. Chem. Phys.* **1982**, *77*, 3654. c) Rassolov, V.; Pople, J. A.; Ratner, M.; Windus, T. L. *J. Chem. Phys.* **1998**, *109*, 1223.

[8] Dunning, T. H.; Hay, P. J. in Methods of Electronic Structure Theory, Vol. 2, Schaefer III, ed., Plenum Press **1977**.

Because the spin densities calculated from the optimized structure are similar to the values calculated from energy calculations on complex **1** using x-ray coordinates, we believe the values from the optimized structure are reliable and report these values in the maintext for consistency with the other calculated values. Spin density calculated from x-ray coordinates for **1** are listed in Table 4, along with spin densities from optimized structures.

Additional energy calculations were run using the same functional as the optimizations with the LANL2TZ(f) for the transition metals, and 6-311G(d,p)[9] basis set for all other atoms. Energy calculations on solid-state structures were run using the same functional and basis set as the energy calculations for the optimized structures.

Other Spectroscopic Measurements. Varian Mercury-300 and Varian Inova-500 were used to collect ^{1}H, ^{13}C, ^{29}Si, and ^{31}P spectra at room temperature unless otherwise noted. ^{1}H and ^{13}C spectra were referenced to residual solvent resonances. ^{29}Si spectra were referenced to external tetramethylsilane (δ = 0 ppm), and ^{31}P spectra were referenced to external 85% phosphoric acid (δ = 0 ppm). IR measurements were obtained on samples prepared as KBr pellets using a Bio-Rad Excalibur FTS 3000 spectrometer. X-band EPR spectra were obtained on a Bruker EMX spectrometer. Spectra were simulated using *Easyspin*[10] program.

Synthesis of {[SiP$^{i\mathrm{Pr}}_3$]Co(PMe$_3$)}BAr$^{\mathrm{F}}_4$ (1).

[SiP$^{i\mathrm{Pr}}_3$]Co(N_2) (30 mg, 0.043 mmol) was dissolved in 8 ml THF. FcBAr$^{\mathrm{F}}_4$ (45.4 mg, 0.043 mmol) was dissolved in 2 ml THF. Both were cooled to -78 ^{o}C. PMe_3 (13μL, 0.043 mmol) was syringed into the [SiP$^{i\mathrm{Pr}}_3$]Co(N_2) solution. The FcBAr$^{\mathrm{F}}_4$ solution was subsequently added to the reaction mixture. The orange solution was stirred at -78 ^{o}C for 10min, and concentrated. The residues were washed with pentane to removed the ferrocene, and the product was extracted into ether, and filtered through celite. Recrystallization by layering pentane over a concentrated ether solution yielded analytically pure product (40 mg, 58%). Recrystallization by slow evaporation of a concentrated ether/methylcyclohexane solution into methylcyclohexane yielded crystals

[9] a) Krishnan, R.; Binkley, J. S.; Seeger, R.; Pople, J. A. *J. CHem. Phys.* **1980**, *72*, 650. b) McLean, A. D.; Chandler, G. S. *J. Chem. Phys.* **1980**, *72*, 5639.

[10] S. Stoll, A. Schweiger, *J. Magn. Reson.* **2006**, *178*, 42.

suitable for x-ray diffraction. ^{1}H NMR (C_6D_6, δ): 18.0, 14.8, 8.7, 7.9, 7.5, 5.6, 4.4, -4.9, -6.6.]). μ_{eff} (Evans' method, C_6D_6:d^8-THF = 10:1, 23 ^{o}C) = 1.8 μ_B. Anal. Calcd for $C_{71}H_{75}SiP_4BF_{24}Co$: C, 53.10; H, 4.71; N. 0.00. Found: C, 52.88; H, 4.42; N, 0.00. UV-VIS (in THF): (nm, ε [mol^{-1} cm^{-1}]), 368 (3100), 403 (2030, sh), 567 (220).

Synthesis of [SiP$^{iPr}_3$]Rh(H)(Cl) (7).

[SiP$^{iPr}_3$]H (220 mg, 0.36 mmol) and [RhCl(COD)] (88 mg, 0.18 mmol) were dissolved in 15 ml of THF and stirred for 3 hr. The solution was concentrated, and the products were extracted into benzene and filtered through celite. The resulting solution was concentrated, washed with pentane (4 X 1ml), and dried to yield the pale yellow product (232 mg, 87%). ^{1}H NMR (C_6D_6, δ): 7.99 (d, *J* = 7.2 Hz, 2H), 7.82 (d, *J* = 7.2 Hz, 1H), 7.38-6.99 (m, 9H), 2.72 (s, 2H), 2.58 (m, *J* = 6.6 Hz, 2H), 2.46 (m, *J* = 7.2 Hz, 2H), 1.82 (q, *J* = 7.2 Hz, 6H), 1.42 (q, *J* = 6.9 Hz, 6H), 1.30 (m, 6H), 1.09-0.95 (m, 12H), 0.54 (q, *J* = 6.9 Hz, 6H), -10.4 (dm, *J* = 143 Hz, 1H). ^{13}C{^{1}H} NMR (C_6D_6, δ): 155.4 (d, *J* = 46 Hz), 152.7 (t, *J* = 22 Hz), 146.4 (t, *J* = 22 Hz), 143.8 (d, *J* = 32 Hz), 133.2 (d, *J* = 19 Hz), 133.1 (t, *J* = 9.6 Hz), 128.8, 128.6, 128.2, 128.0, 126.6 (d, *J* = 5.0 Hz), 29.7 (m), 28.9 (m), 21.4, 19.8, 19.2, 18.8, 18.5. ^{31}P{^{1}H} NMR (C_6D_6, δ): 57.2 (d, *J* = 109 Hz, 2P) 47.9 (br, 1P). IR (KBr, cm^{-1}): 2037 (ν[Rh-H]).

Synthesis of [SiP$^{iPr}_3$]Rh(N$_2$) (5).

[SiP$^{iPr}_3$]Rh(H)(Cl) (150 mg, 0.20 mmol) was dissolved in 12 ml of THF. MeMgCl (75 μL, 0.22 mmol, 3M sln) was diluted with 3 ml of THF. Both were cooled to -78 ^{o}C. The MeMgCl solution was added dropwise to the pale yellow solution of the complex, resulting in a color change to red/orange. The resulting mixture was stirred for 15 min at -78 ^{o}C, and then stirred at RT for 1.5 hr, yielding a dark green solution. The solution was concentrated, and the product was extracted into a 2:1 solution of benzene:pentane, and filtered through celite. Concentration of the solution yielded the product (141 mg, 97%). ^{1}H NMR (C_6D_6, δ): 7.98 (d, *J* = 7.2 Hz, 3H), 7.30 (d, *J* = 7.5 Hz, 3H), 7.19-7.04 (m, 6H), 2.44 (m, 6H), 1.06 (m, 18H), 0.72 (m, 18H). ^{13}C NMR (C_6D_6, δ): 155.6 (m), 145.3 (m), 132.5 (m), 128.0, 128.0, 126.2, 28.9, 18.8, 18.7. ^{31}P NMR (C_6D_6, δ): 59.5 (d, *J* = 160 Hz).

Synthesis of [SiP$^{i\mathrm{Pr}}_3$]Rh(PMe$_3$) (8).

[SiP$^{i\mathrm{Pr}}_3$]Rh(N$_2$) (90 mg, 0.13 mmol) was dissolved in 10 ml THF. The solution was cooled to -78 ^{o}C and PMe$_3$ (26μL, 0.25 mmol) was syringed in. The solution was stirred at room temperature for 5 min, and concentrated. Trituration with hexamethyldisiloxane yielded a yellow powder (95 mg, 95%). ^{1}H NMR (C$_6$D$_6$, δ): 8.17 (d, *J* = 6.9 Hz, 3H), 7.45 (d, *J* = 7.8 Hz, 3H), 7.23 (t, *J* = 7.2 Hz, 3H), 7.11 (t, *J* = 7.2 Hz, 3H), 2.30 (br, 6H), 1.65 (d, *J* = 4.8 Hz, 3H), 0.97 (br, 18H), 0.80 (br, 18H). ^{13}C NMR (C$_6$D$_6$, δ): 156.6 (m), 148.3 (m), 132.3, 128.4 (br), 128.0, 126.1, 29.9, 28.9, 20.2, 18.6. ^{31}P NMR (C$_6$D$_6$, δ): 54.3 (dd, *J* = 153, 39 Hz, 3P), -29.5 (dq, *J* = 106 Hz, 39 Hz, 1P).

Synthesis of {[SiP$^{i\mathrm{Pr}}_3$]Rh(PMe$_3$)}BAr$^{F}_4$ (2).

[SiP$^{i\mathrm{Pr}}_3$]Rh(PMe$_3$) (50 mg, 0.064 mmol) was dissolved in 8 ml THF. FcBAr$^{F}_4$ (67 mg, 0.064 mmol) was dissolved in 3 ml THF. Both were cooled to -78 ^{o}C. The FcBAr$^{F}_4$ solution was added dropwise to the [SiP$^{i\mathrm{Pr}}_3$]Rh(PMe$_3$) solution, causing a color change to green. The reaction mixture was stirred for 10 min, after which the reaction mixture was stirred for 30 min. The mixture was concentrated, and the residues were washed with pentane. The product was extracted into ether, and filtered through celite. Recrystallization from layering pentane over a concentrated ether solution yielded crystals suitable for x-ray diffraction (69 mg, 66%). ^{1}H NMR (C$_6$D$_6$:d^8-THF = 10:1, δ): 12.0, 9.8, 8.4, 7.7, 5.3, -0.1.]). μ_{eff} (Evans' method, C$_6$D$_6$:d^8-THF = 10:1, 23 ^{o}C) = 1.6 μ_B. Anal. Calcd for C$_{71}$H$_{75}$SiP$_4$BF$_{24}$Rh: C, 51.68; H, 4.58; N. 0.00. Found: C, 51.33; H, 4.48; N, 0.00. UV-VIS (in THF): (nm, ε [mol^{-1} cm^{-1}]), 307 (5900, sh), 639 (320).

Synthesis of [SiP$^{i\mathrm{Pr}}_3$]Ir(PMe$_3$) (9).

[SiP$^{i\mathrm{Pr}}_3$]Ir(N$_2$) (90 mg, 0.11 mmol) was dissolved in 6 ml THF. The solution was cooled to -78 ^{o}C and PMe$_3$ (34μL, 0.033 mmol) was syringed into the reaction mixture. The reaction mixture was stirred for 5 min at -78^{o}C and concentrated. The residues were extracted into ether, filtered through celite, and concentrated. Trituration with hexamethyldisiloxane resulted in a yellow powder (95 mg, 99%). ^{1}H NMR (C$_6$D$_6$, δ): 8.25 (d, *J* = 7.5 Hz, 3H), 7.42 (d, *J*= 8 Hz, 3H), 7.20 (t, *J* = 7 Hz, 3H), 7.07 (t, *J* = 7.5 Hz, 3H), 2.38 (s, 6H), 1.88 (d, *J* = 6.0 Hz, 3H), 0.94 (s, 18H), 0.75 (s, 18H). ^{13}C NMR (C$_6$D$_6$, δ): 155.5 (m), 149.8 (m), 131.9 (q, *J* = 6.3 Hz), 127.7, 126.0,

31.6 (d, *J* = 22.1 Hz), 31.4 (br), 20.0, 18.6. ^{31}P NMR (C_6D_6, δ): 27.8 (br, 3P), -74.0 (q, *J* = 27.2 Hz, 1P).

Synthesis of {[SiP$^{i\text{Pr}}_3$]Ir(PMe$_3$)}BAr$^F_4$ (3).

[SiP$^{i\text{Pr}}_3$]Ir(PMe$_3$) (30 mg, 0.038 mmol) was dissolved in 5 ml Et_2O. FcBAr$^F_4$ (40 mg, 0.038 mmol) was dissolved in 2 ml Et_2O. Both were cooled to -78 ^{o}C. The FcBAr$^F_4$ solution was added dropwise to the [SiP$^{i\text{Pr}}_3$]Ir(PMe$_3$) solution. An immediate color change from yellow to purple resulted. The reaction mixture was stirred for 2 min at -78 ^{o}C, and was stirred at 5 min at RT. The reaction mixture was concentrated and the residues were washed with pentane. The solids were extracted into ether, filtered through celite, and concentrated to yield the purple product. Layering pentane over a concentrated ether solution resulted in purple crystals (58 mg, 87%). Crystals of the product with OTf^- as the anion, [SiP$^{i\text{Pr}}_3$]Ir(PMe$_3$)}OTf (**3'**), which was synthesized by the addition of AgOTf to [SiP$^{i\text{Pr}}_3$]Ir(PMe$_3$) in THF, were obtained from recrystallization by layering pentane over a concentrated dichloromethane solution. These crystals were amenable to X-ray diffraction. ^{1}H NMR (C_6D_6:d^8-THF = 10:1, δ): 15.9, 10.9, 9.1, 8.3, 7.7, 5.9, -0.5.]). μ_{eff} (Evans' method, C_6D_6:d^8-THF = 10:1, 23 ^{o}C) = 1.7 μ_B. Anal. Calcd for $C_{71}H_{75}SiP_4BF_{24}Ir$: C, 49.03; H, 4.35; N. 0.00. Found: C, 49.47; H, 4.56; N, 0.00. UV-VIS (in THF): (nm, ε [mol^{-1} cm^{-1}]), 366 (138, sh), 482 (360, sh), 566 (470).

Figure 1. ^{1}H NMR spectrum of {[SiP$^{i\mathrm{Pr}}_{3}$]Co(PMe$_3$)}BAr$^{\mathrm{F}}_{4}$ (1).

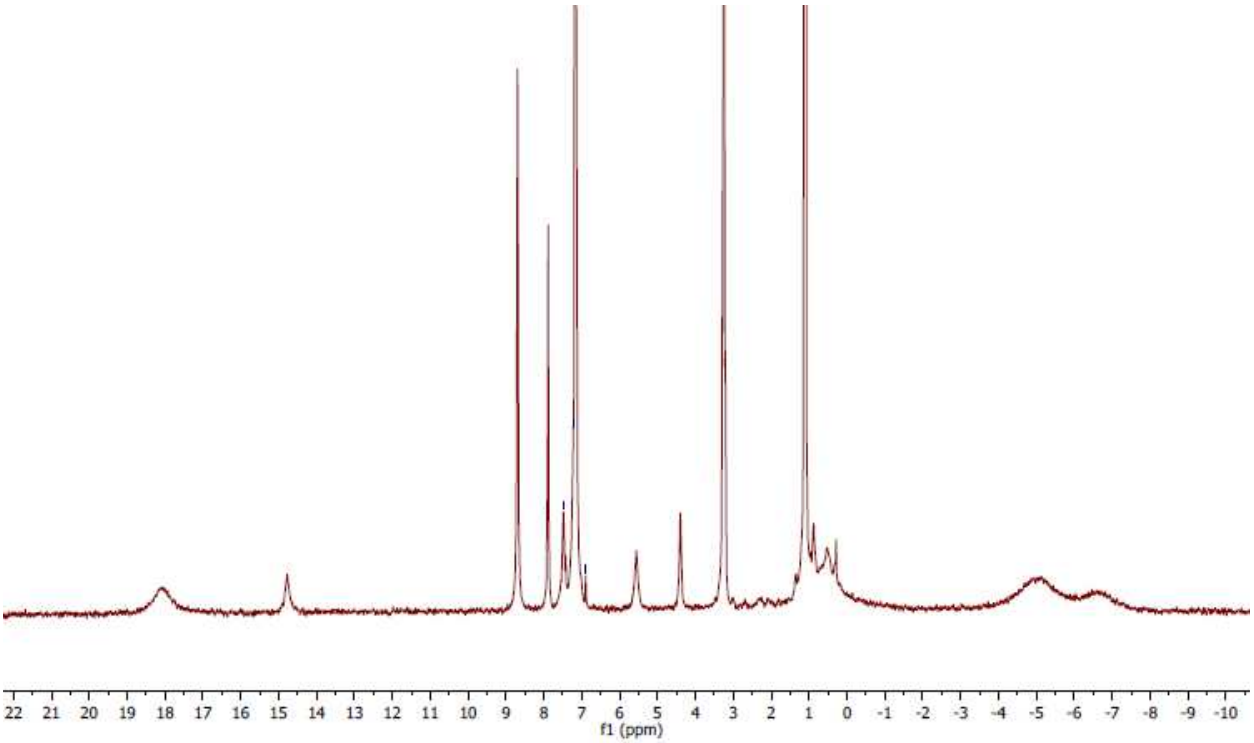

Figure 2. NMR spectra of [SiP$^{i\mathrm{Pr}}_{3}$]Rh(H)(Cl) (7).

^{1}H

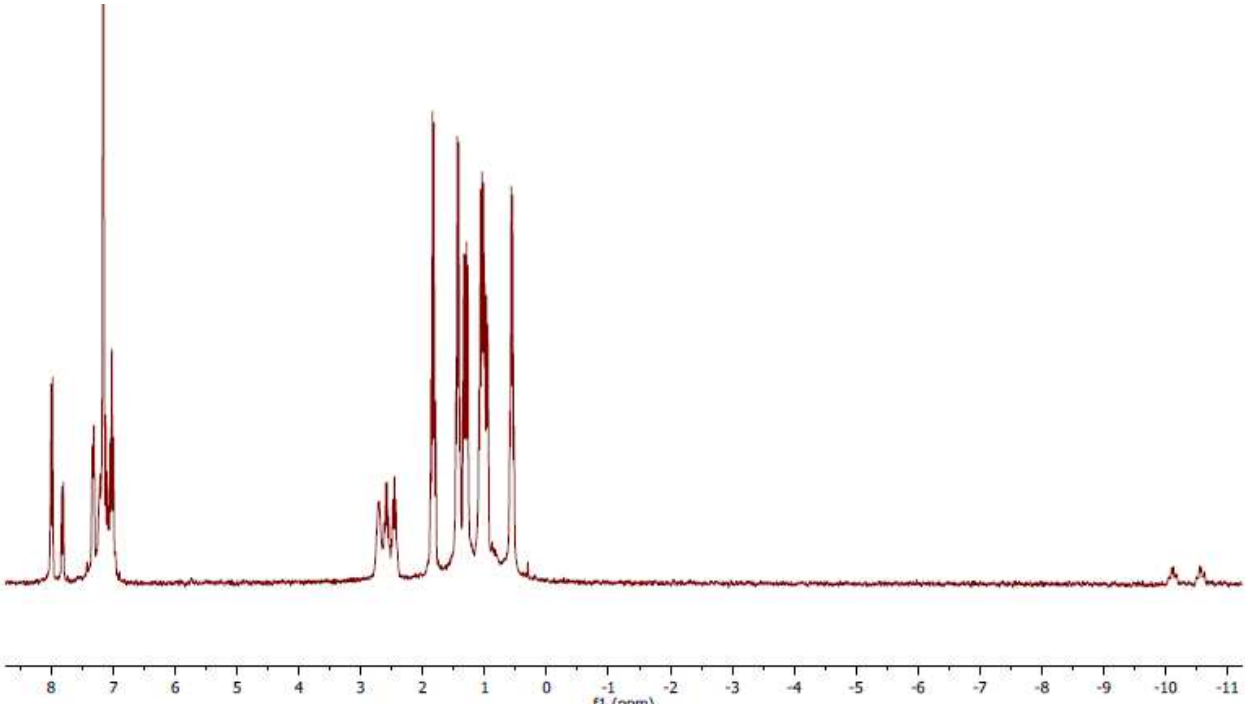

^{13}C

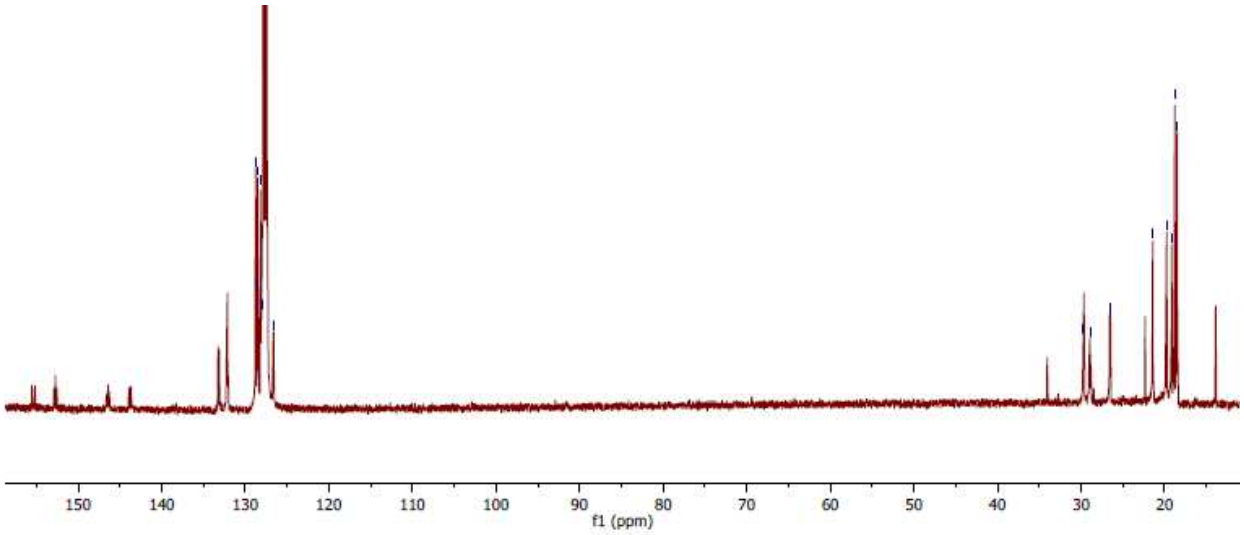
150
140
130
120
110
100
90
80
70
60
50
40
30
20
f1 (ppm)

^{31}P

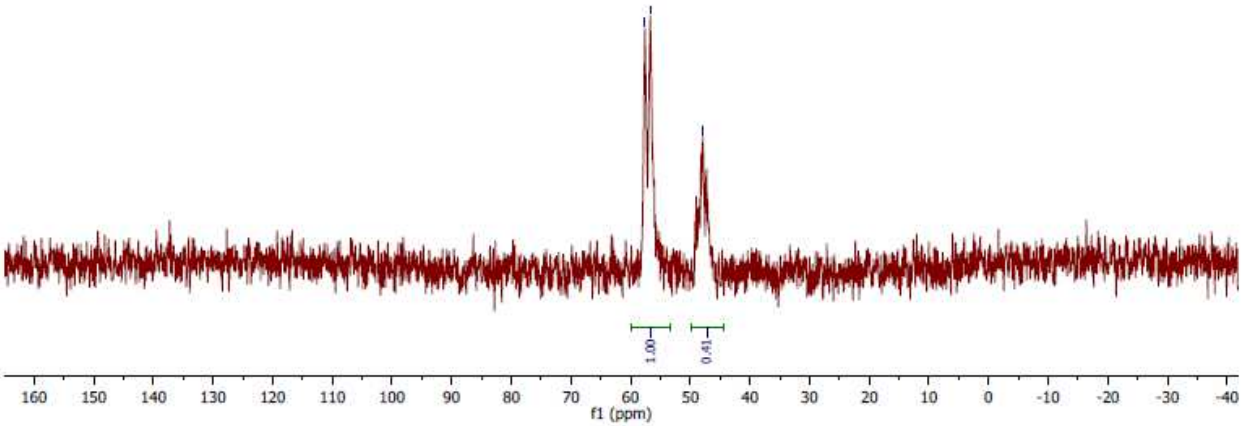
1.00
0.41
160
150
140
130
120
110
100
90
80
70
60
50
40
30
20
10
0
-10
-20
-30
-40
f1 (ppm)

Figure 3. NMR spectra of [SiP$^{iPr}_3$]Rh(N_2) (5).

^{1}H

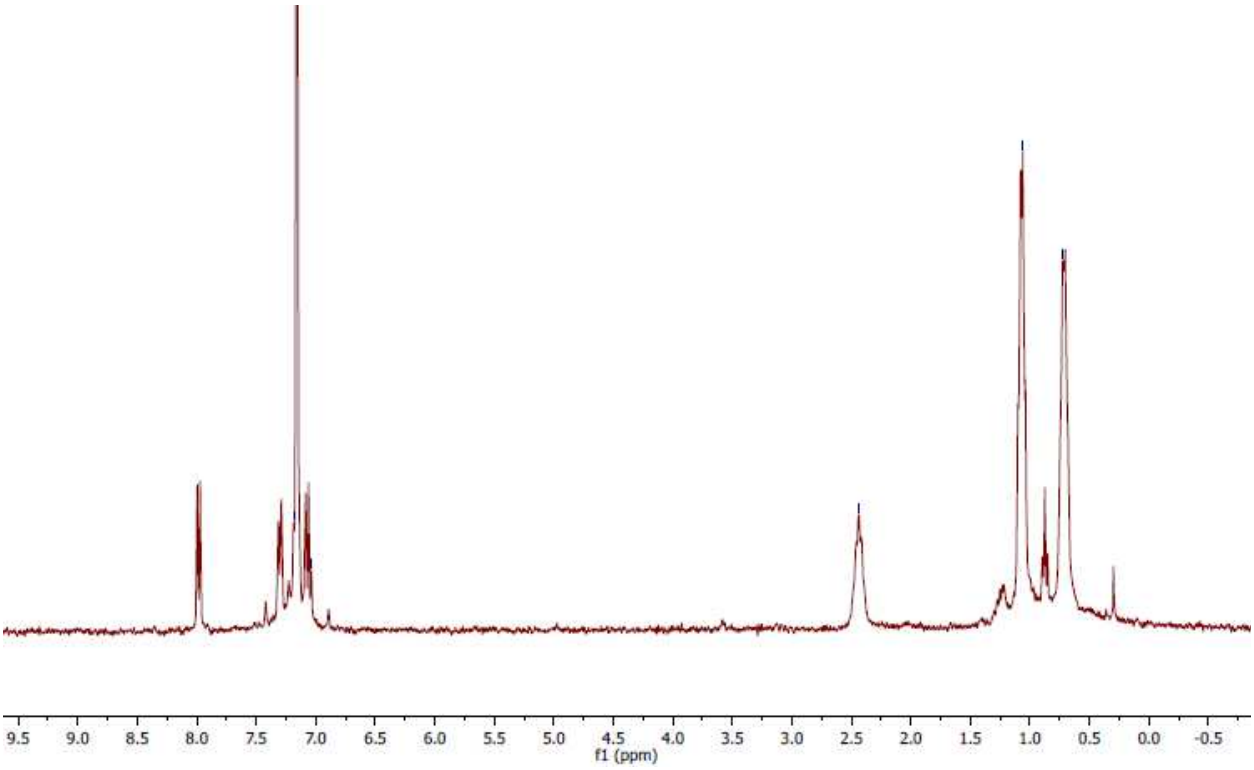

^{13}C

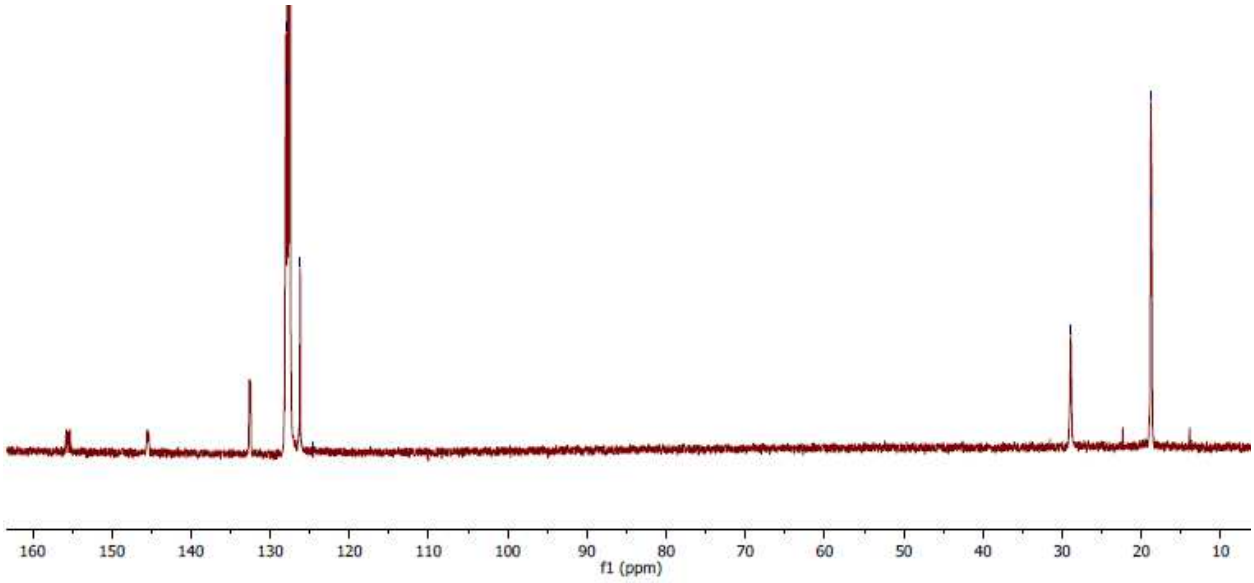

^{31}P

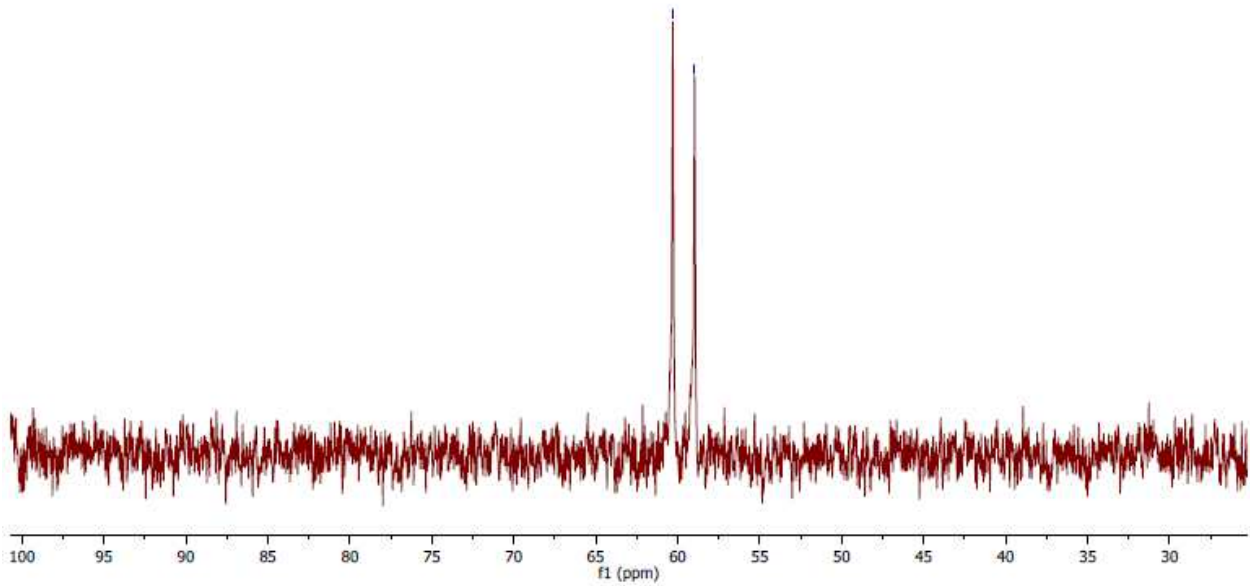

Figure 4. NMR spectra of [SiP$^{iPr}_3$]Rh(PMe$_3$) (8).

^{1}H

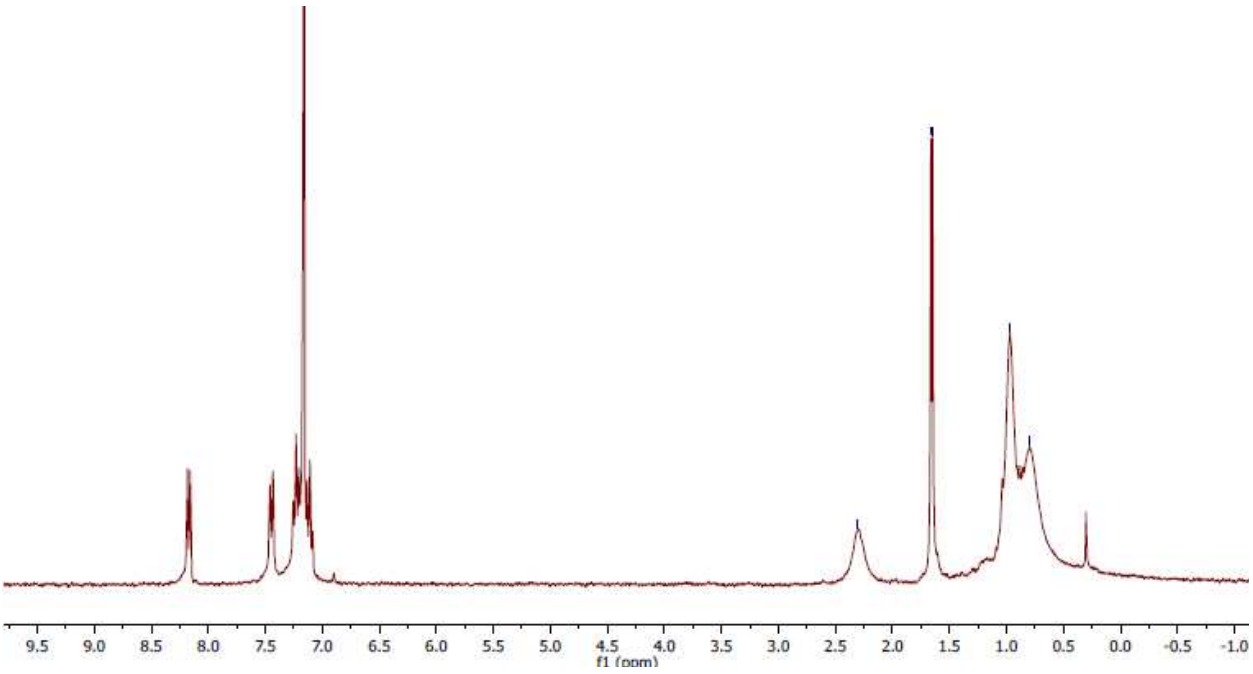

^{13}C

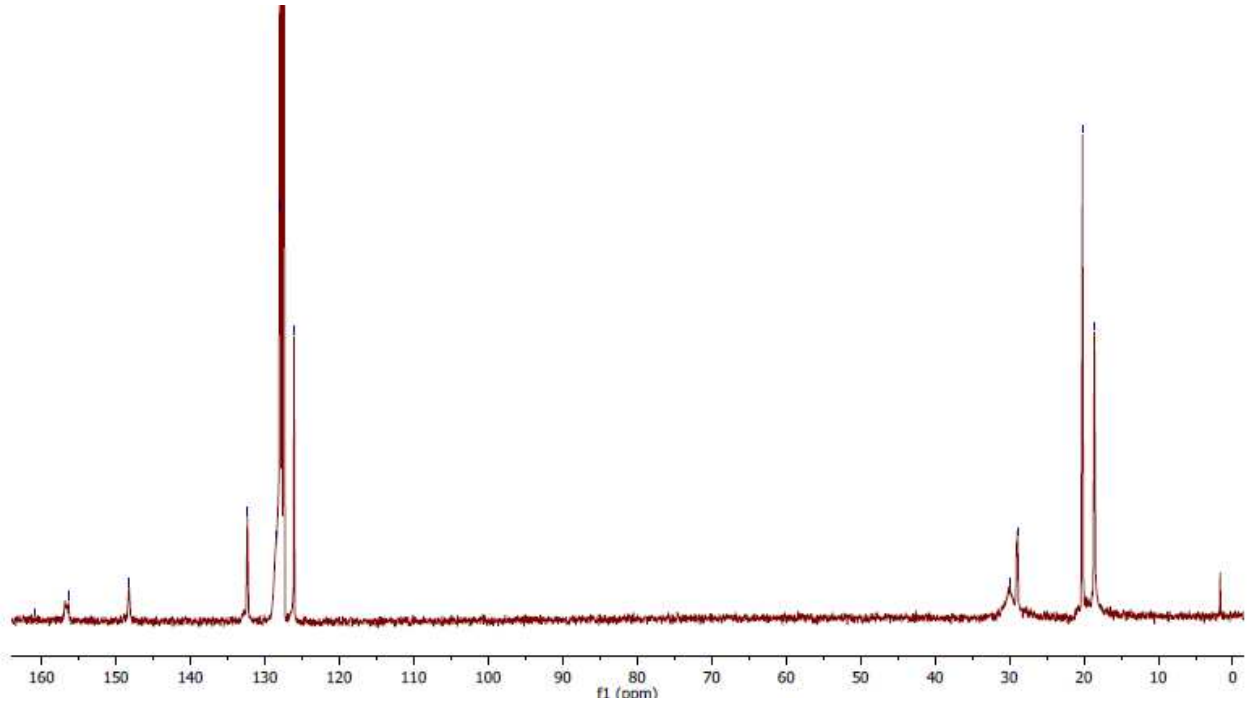
160
150
140
130
120
110
100
90
80
70
60
50
40
30
20
10
0
f1 (ppm)

^{31}P

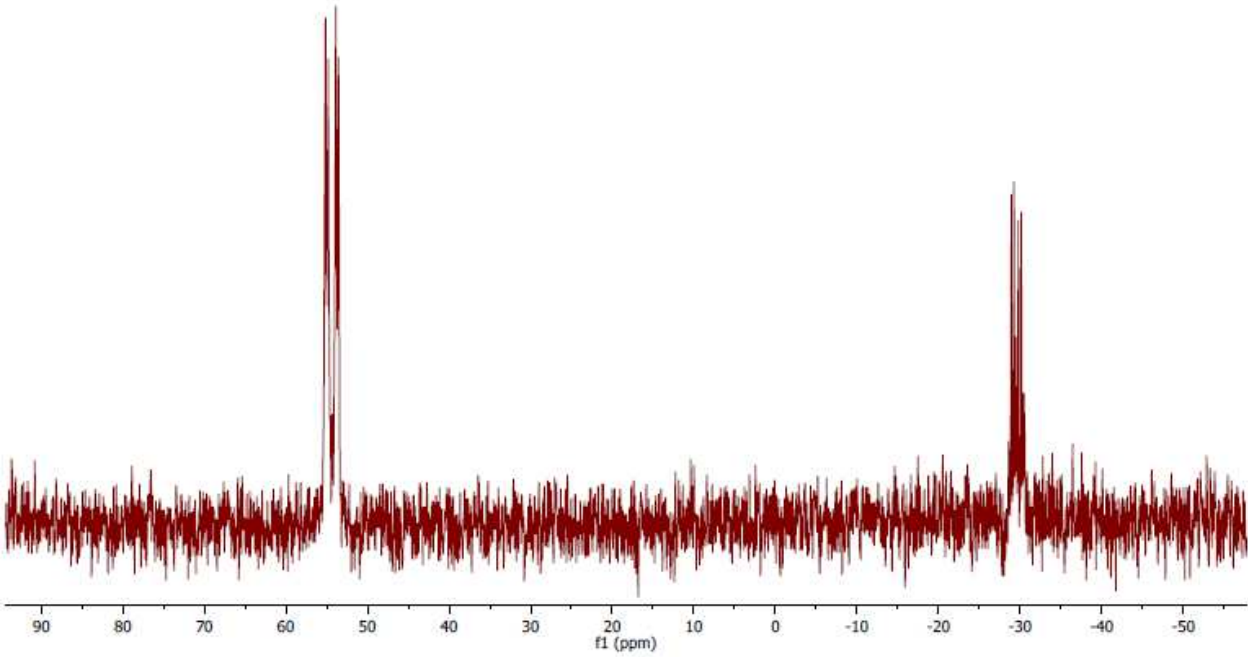
90
80
70
60
50
40
30
20
10
0
-10
-20
-30
-40
-50
f1 (ppm)

Figure 5. ^{1}H NMR spectrum of {[SiP$^{i\mathrm{Pr}}_{3}$]Rh(PMe$_3$)}BAr$^{F}_{4}$ (2).

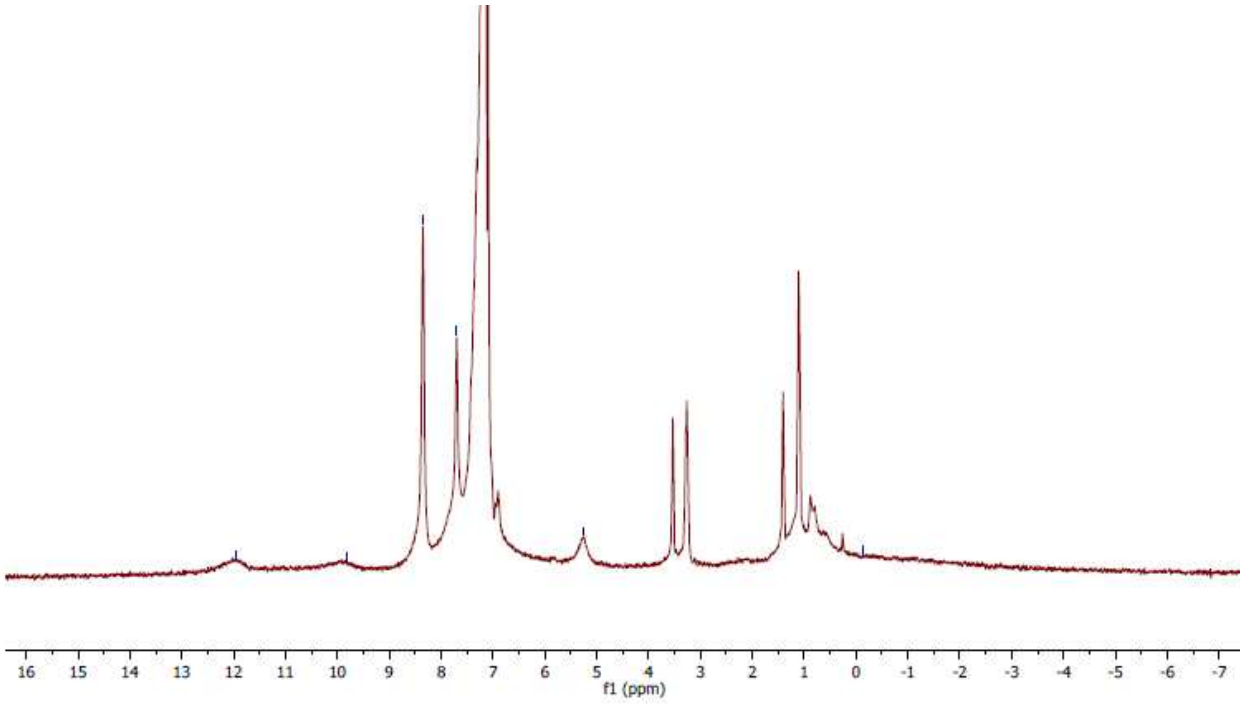

Figure 6. NMR spectra of [SiP$^{i\mathrm{Pr}}_{3}$]Ir(PMe$_3$) (9).

^{1}H

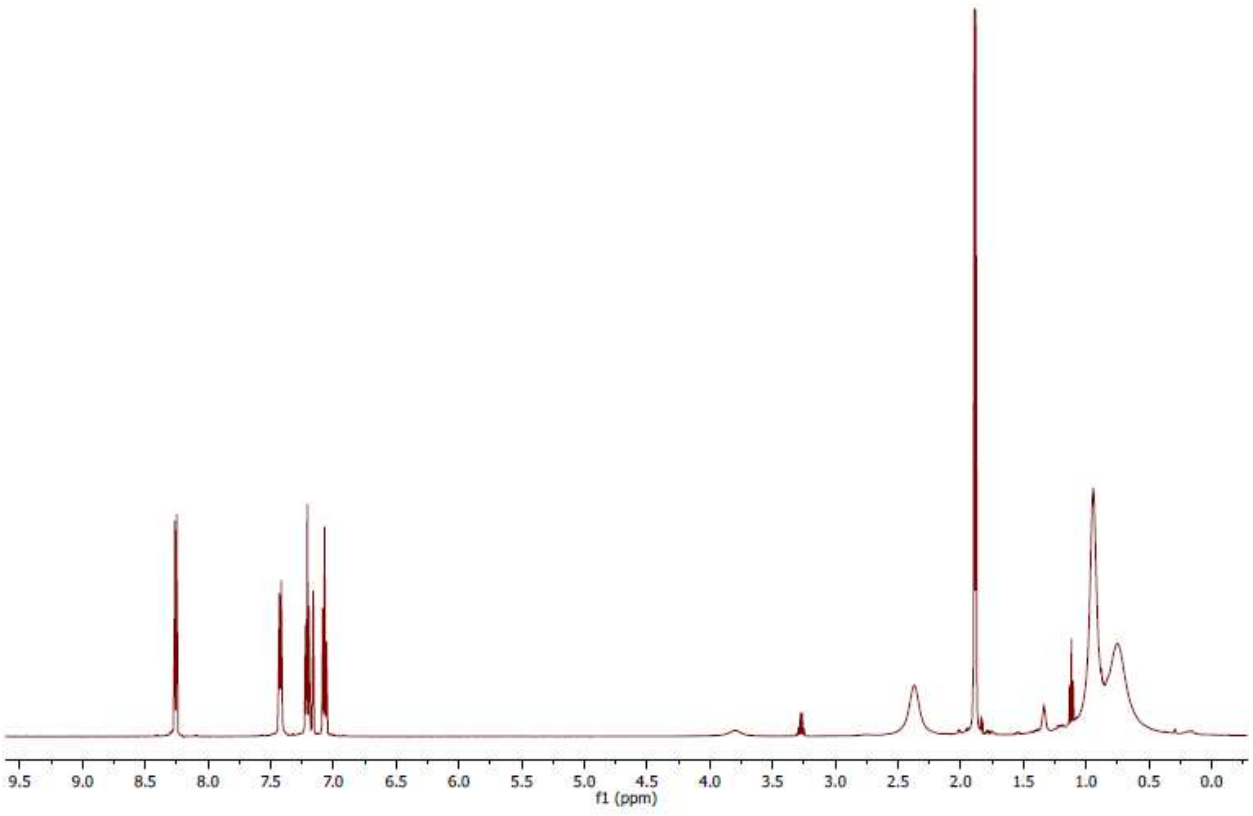

^{13}C

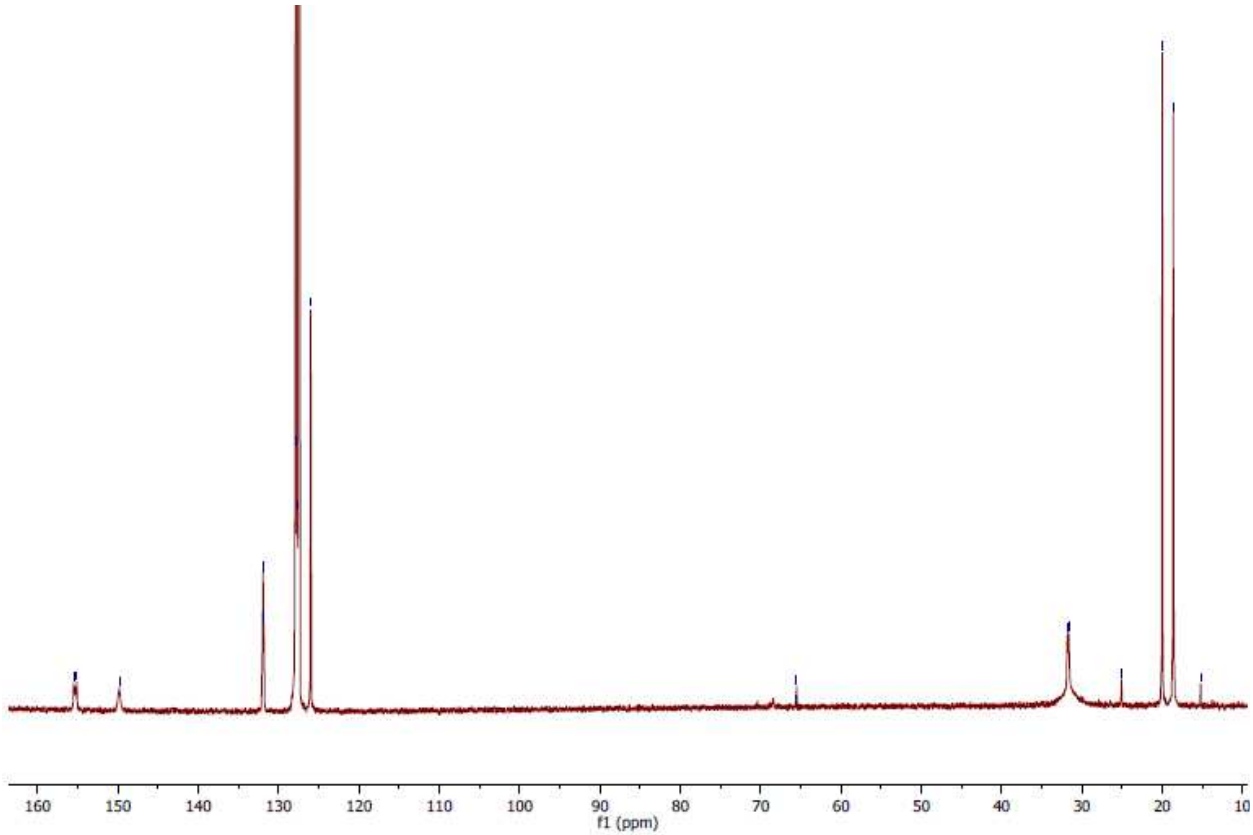
160
150
140
130
120
110
100
90
80
70
60
50
40
30
20
10
f1 (ppm)

^{31}P

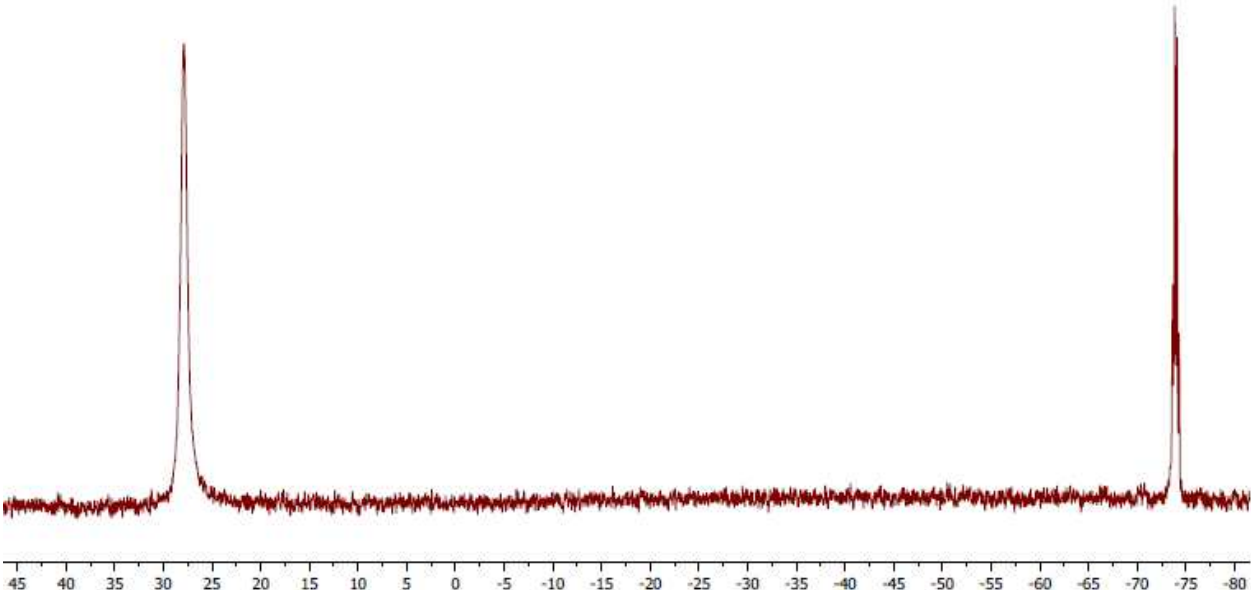
45
40
35
30
25
20
15
10
5
0
-5
-10
-15
-20
-25
-30
-35
-40
-45
-50
-55
-60
-65
-70
-75
-80

Figure 7. ^{1}H NMR spectrum of {[SiP$^{i\text{Pr}}_3$]Ir(PMe$_3$)}BAr$^{F}_4$ (3).

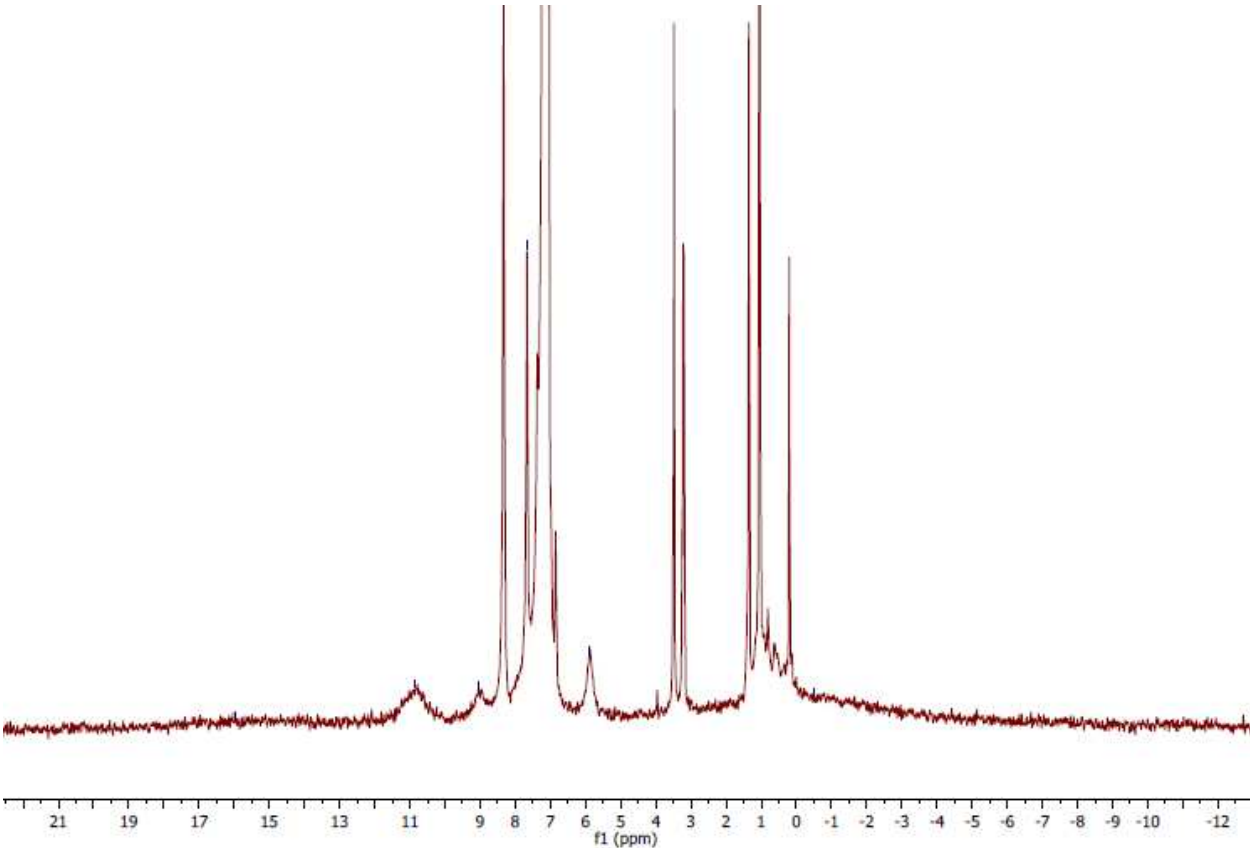

Figure 8. Cyclic Voltammogram of {[SiP$^{i\text{Pr}}_3$]Co(PMe$_3$)}BAr$^{F}_4$ (1).

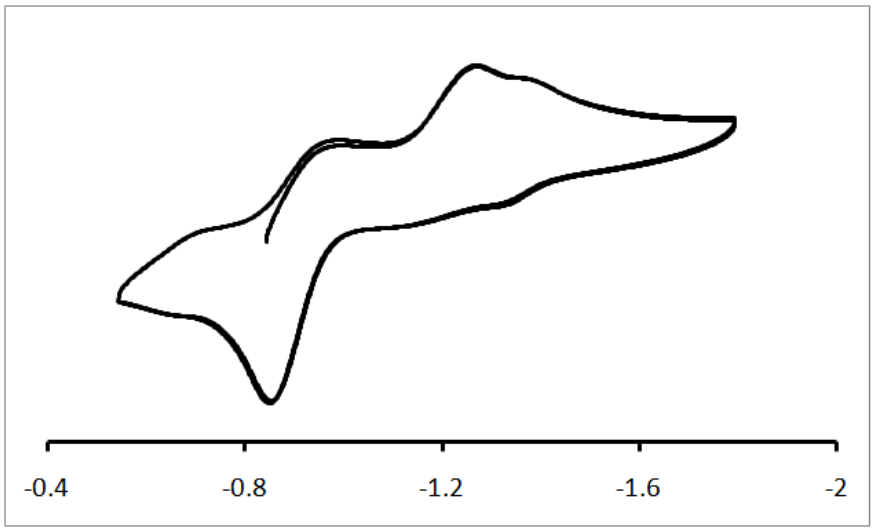

Figure 9. Cyclic Voltammogram of [SiP$^{i\text{Pr}}_3$]Rh(PMe$_3$) (8).

The irreversibility observed in this CV compared to the CV for the Rh and Ir species (shown below) is due to irreversible loss of PMe_3 observed in the Co complex **1** upon reduction. In Rh and Ir, reduction/oxidation does not result in loss of PMe_3.

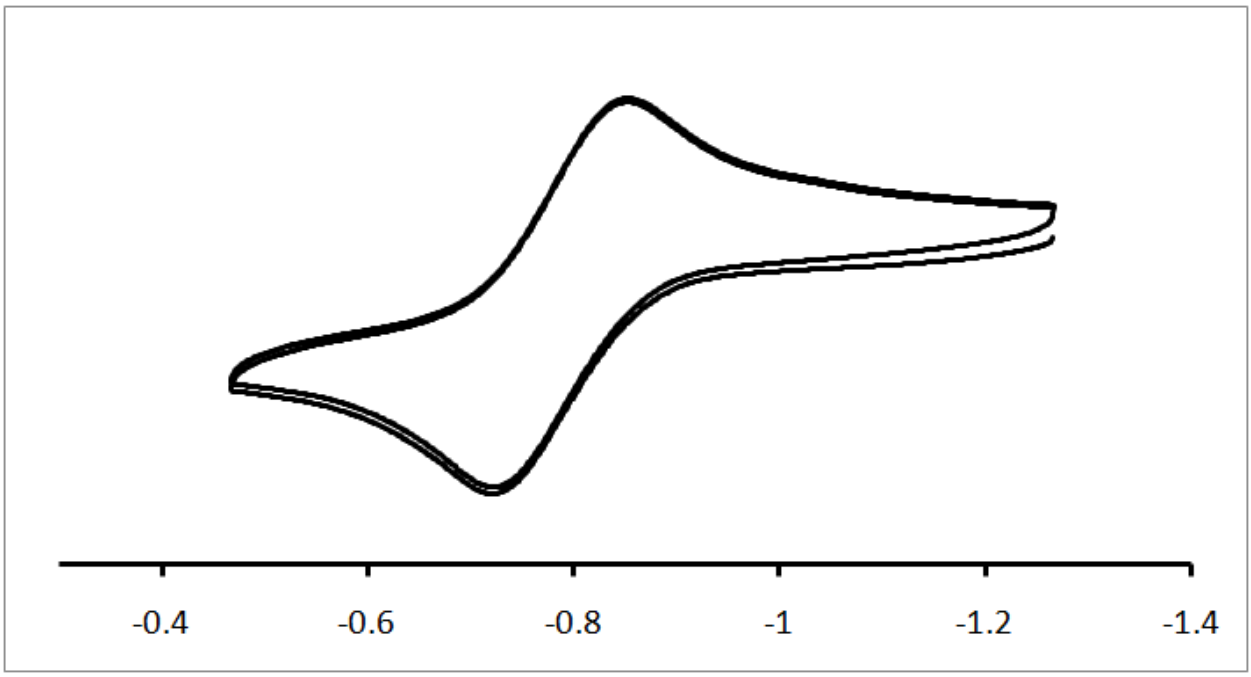

Figure 10. Cyclic Voltammogram of [SiP$^{iPr}_3$]Ir(PMe$_3$) (8).

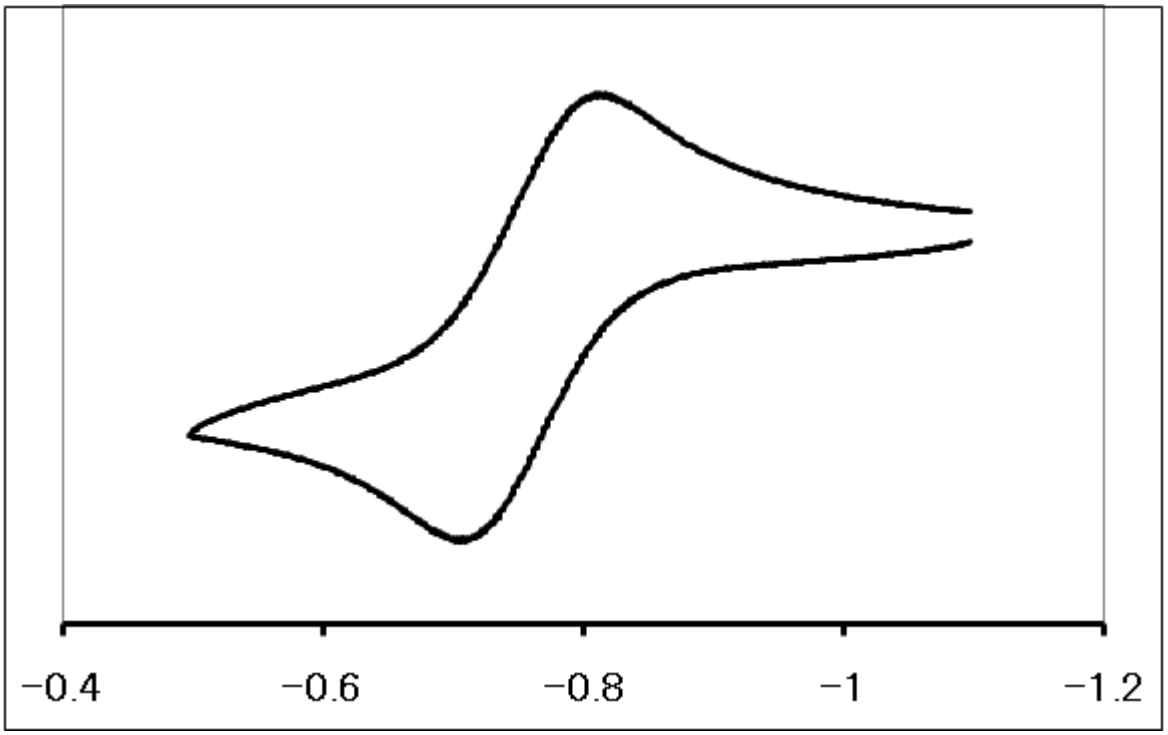

Figure 11. 77 K EPR spectrum of {[SiP$^{iPr}_3$]Co(PMe$_3$)}BAr$^F_4$ (1).

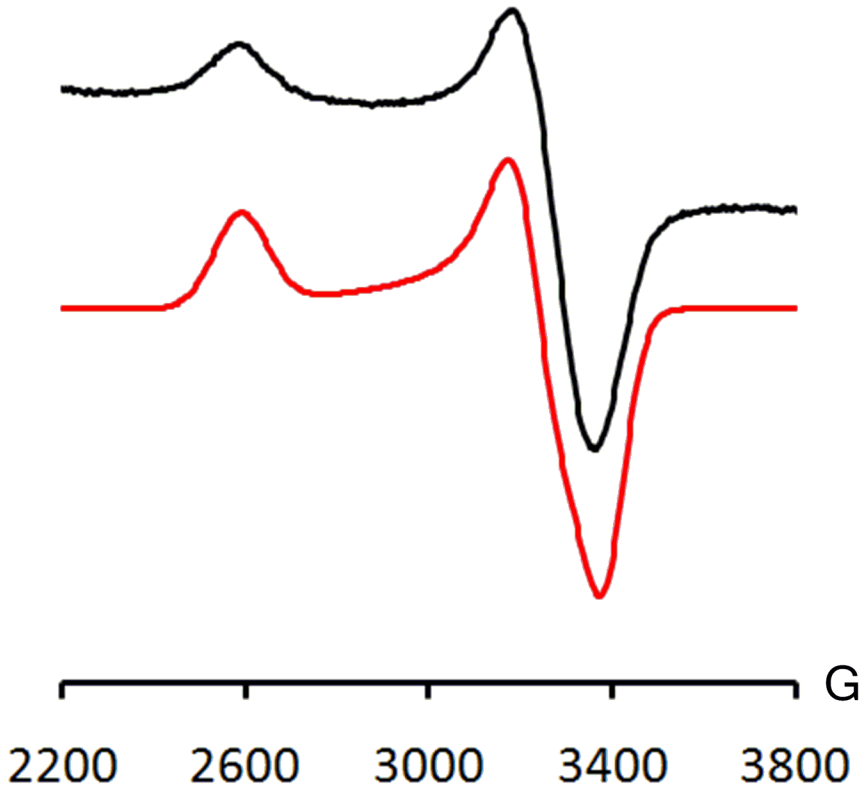

Experimental parameters; Microwave power, 0.814 mW; microwave frequency, 9.418 GHz; modulation amplitude, 2 G; gain, 2000.

Simulation parameters: g_x = 2.60, g_y = 2.08, g_z = 1.99; Linewidth, lw = 1; HStrain; W_x = 500 MHz, W_y = 350 MHz, W_z = 300 MHz.

Figure 12. RT EPR spectrum of {[SiP$^{i\text{Pr}}_3$]Rh(PMe$_3$)}BAr$^{\text{F}}_4$ (2).

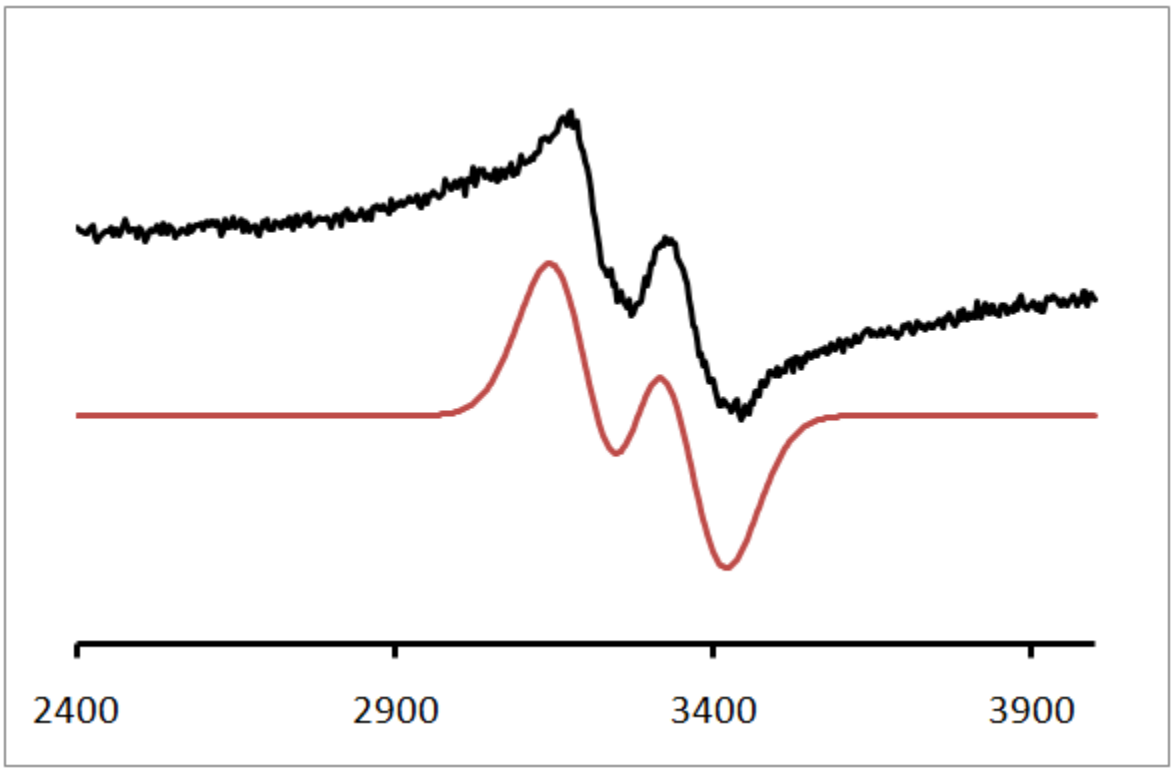

Experimental parameters; Microwave power, 2.036 mW; microwave frequency, 9.647 GHz; modulation amplitude, 2 G; gain, 20000.

Simulation parameters: g = 2.10, g_y . Linewidth, lw =15; For 1 P atom, A(P) = 450 MHz.

Figure 13. 77 K EPR spectrum of {[SiP$^{iPr}_3$]Rh(PMe$_3$)}BAr$^F_4$ (2).

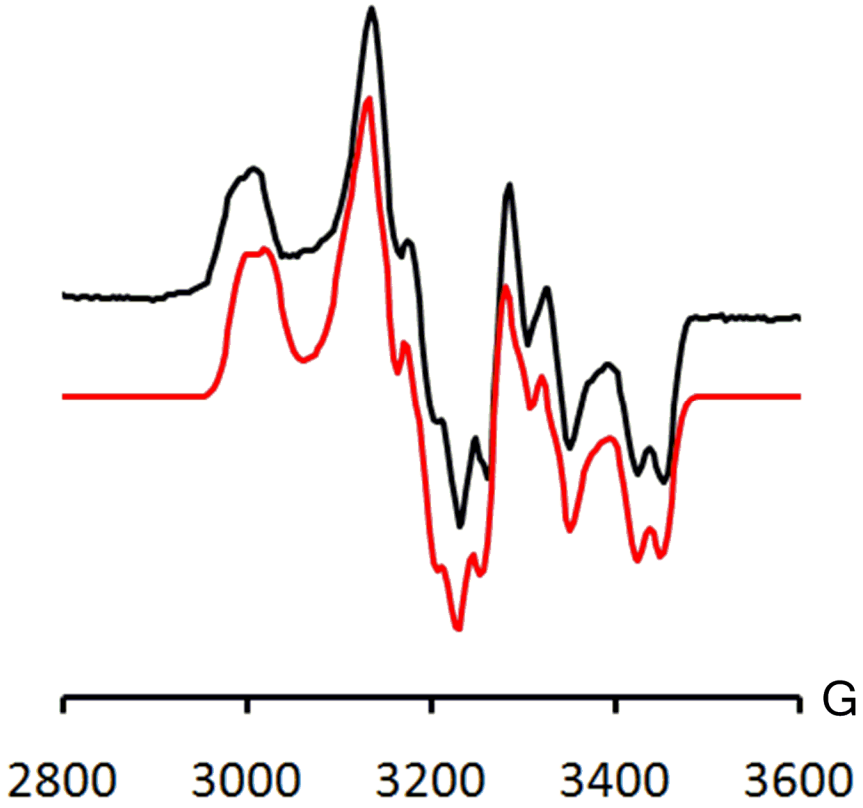

Experimental parameters; Microwave power, 0.807 mW; microwave frequency, 9.417 GHz; modulation amplitude, 2 G; gain, 2000.

Simulation parameters: g_x = 2.205, g_y = 2.087, g_z = 2.025; For one P atom, $A_x(^{31}P)$ = 360 MHz, $A_y(^{31}P)$ = 430 MHz, $A_z(^{31}P)$ = 550 MHz ; For one atom of I = ½ (P or Rh), A_x = 90 MHz, A_y = 115 MHz, A_z = 80 MHz ; For one atom of I = ½ (P or Rh), A_x = 1 MHz, A_y = 50 MHz, A_z = 1 MHz. Linewidth, lw =1, HStrain, W_x = 95 MHz, W_y = 50 MHz, W_z = 68 MHz.

Figure 14. RT EPR spectrum of {[SiP$^{iPr}_3$]Ir(PMe$_3$)}BAr$^F_4$ (3).

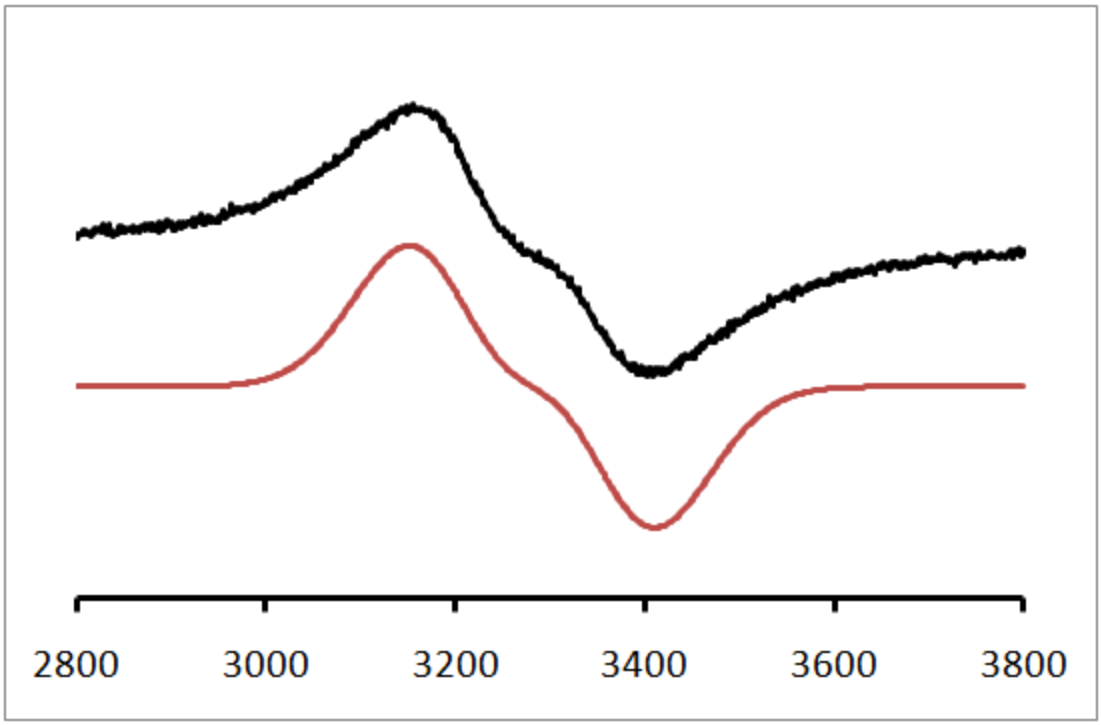

Experimental parameters; Microwave power, 0.401 mW; microwave frequency, 9.855 GHz; modulation amplitude, 10 G; gain, 1000.

Simulation parameters: g = 2.145, g_y . Linewidth, lw =17; For 1 P atom, A(P) = 400 MHz.

Figure 15. 77K EPR spectrum of {[SiP$^{i\mathrm{Pr}}_3$]Ir(PMe$_3$)}BAr$^{\mathrm{F}}_4$ (3).

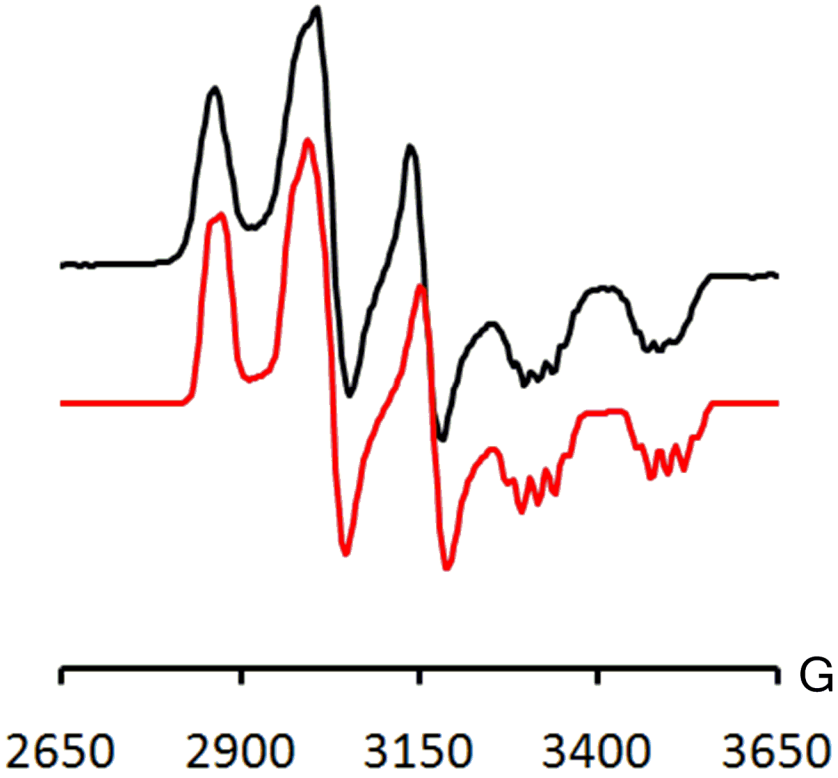

Experimental parameters; Microwave power, 0.813 mW; microwave frequency, 9.419 GHz; modulation amplitude, 2 G; gain, 2000.

Simulation parameters: g_x = 2.300, g_y = 2.170, g_z = 1.975; For one P atom, $A_x(^{31}P)$ = 370 MHz, $A_y(^{31}P)$ = 430 MHz, $A_z(^{31}P)$ = 500 MHz ; For one P atom, A_x (^{31}P) = 70 MHz, A_y (^{31}P) = 30 MHz, A_z (^{31}P) = 50 MHz ; For one Ir atom, A_x (Ir) = 1 MHz, A_y = 1 MHz, A_z = 65 MHz. Linewidth, lw =1, HStrain, W_x = 35 MHz, W_y = 90 MHz, W_z = 70 MHz.

Table 1. Crystal data and structure refinement for {**[SiP$^{iPr}_3$]Co(PMe$_3$)**}**BAr$^F_4$ (1)**

Identification code	ayt17	
Empirical formula	C71 H75 B Co F24 P4 Si	
Formula weight	1606.02	
Temperature	100(2) K	
Wavelength	0.71073 Å	
Crystal system	Monoclinic	
Space group	C2/c	
Unit cell dimensions	a = 38.7112(11) Å	□= 90°.
	b = 14.8630(4) Å	□= 110.296(2).
	c = 29.3525(8) Å	□ = 90°.
Volume	4983.9(9) Å^3	
Z	8	
Density (calculated)	1.347 Mg/m^3	
Absorption coefficient	0.407 mm^{-1}	
F(000)	6584	
Crystal size	0.17 x 0.13 x 0.12 mm^3	
Theta range for data collection	2.17 to 24.89°.	
Index ranges	-48<=h<=47, -18<=k<=18, -36<=l<=36	
Reflections collected	150225	
Independent reflections	16140 [R(int) = 0.0918]	
Completeness to theta = 33.13°	99.6 %	
Absorption correction	none	
Max. and min. transmission		
Refinement method	Full-matrix least-squares on F^2	
Data / restraints / parameters	16140 / 415 / 1047	
Goodness-of-fit on F^2	1.127	
Final R indices [I>2sigma(I)]	R1 = 0.0587, wR2 = 0.1510	
R indices (all data)	R1 = 0.1009, wR2 = 0.1763	
Largest diff. peak and hole	1.047 and -0.693 e.Å^{-3}	

Figure 16. Solid-state Structure of {**[SiP$^{i\mathrm{Pr}}_3$]Co(PMe$_3$)}BAr$^{\mathrm{F}}_4$ (1)**.

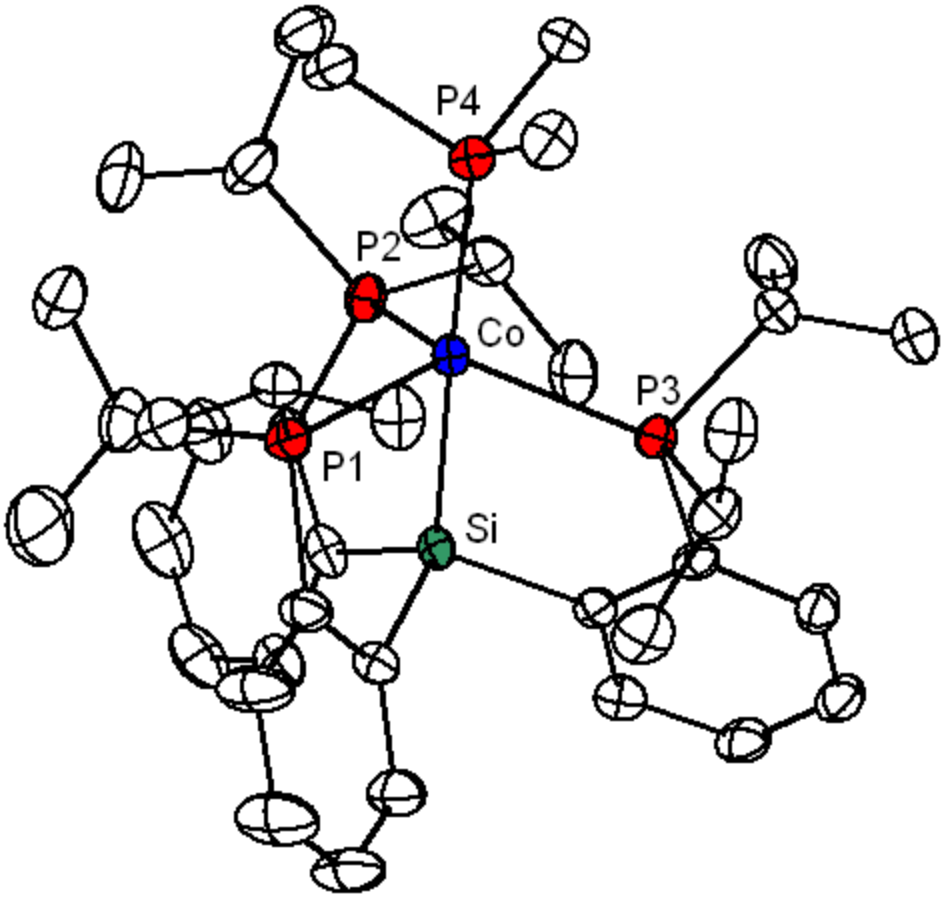

Hydrogen atoms, BAr$^{\mathrm{F}}_4$ anion, and solvent molecule removed for clarity.

Table 2. Crystal data and structure refinement for {**[SiP$^{iPr}_3$]Rh(PMe$_3$)}BAr$^F_4$ (2)**

Identification code	ayt16try2	
Empirical formula	C71 H75 B F24 P4 Rh Si	
Formula weight	1650.00	
Temperature	100(2) K	
Wavelength	0.71073 Å	
Crystal system	Monoclinic	
Space group	C2/c	
Unit cell dimensions	a = 38.898(2) Å	□= 90°.
	b = 14.9266(10) Å	□= 110.083(3)°.
	c = 29.4282(19) Å	□ = 90°.
Volume	16047.7(18) Å^3	
Z	8	
Density (calculated)	1.366 Mg/m^3	
Absorption coefficient	0.401 mm^{-1}	
F(000)	6728	
Crystal size	0.36 x 0.23 x 0.08 mm^3	
Theta range for data collection	2.16 to 27.83°.	
Index ranges	-55<=h<=55, -21<=k<=21, -42<=l<=42	
Reflections collected	211474	
Independent reflections	24573 [R(int) = 0.0691]	
Completeness to theta = 33.13°	99.7 %	
Absorption correction	none	
Max. and min. transmission		
Refinement method	Full-matrix least-squares on F^2	
Data / restraints / parameters	24573 / 816 / 1149	
Goodness-of-fit on F^2	0.918	
Final R indices [I>2sigma(I)]	R1 = 0.0550, wR2 = 0.1662	
R indices (all data)	R1 = 0.0848, wR2 = 0.1931	
Largest diff. peak and hole	2.569 and -0.555 e.Å^{-3}	

Figure 17. Solid-state Structure of {**[SiP$^{i\mathrm{Pr}}_3$]Rh(PMe$_3$)}BAr$^{\mathrm{F}}_4$ (2)**.

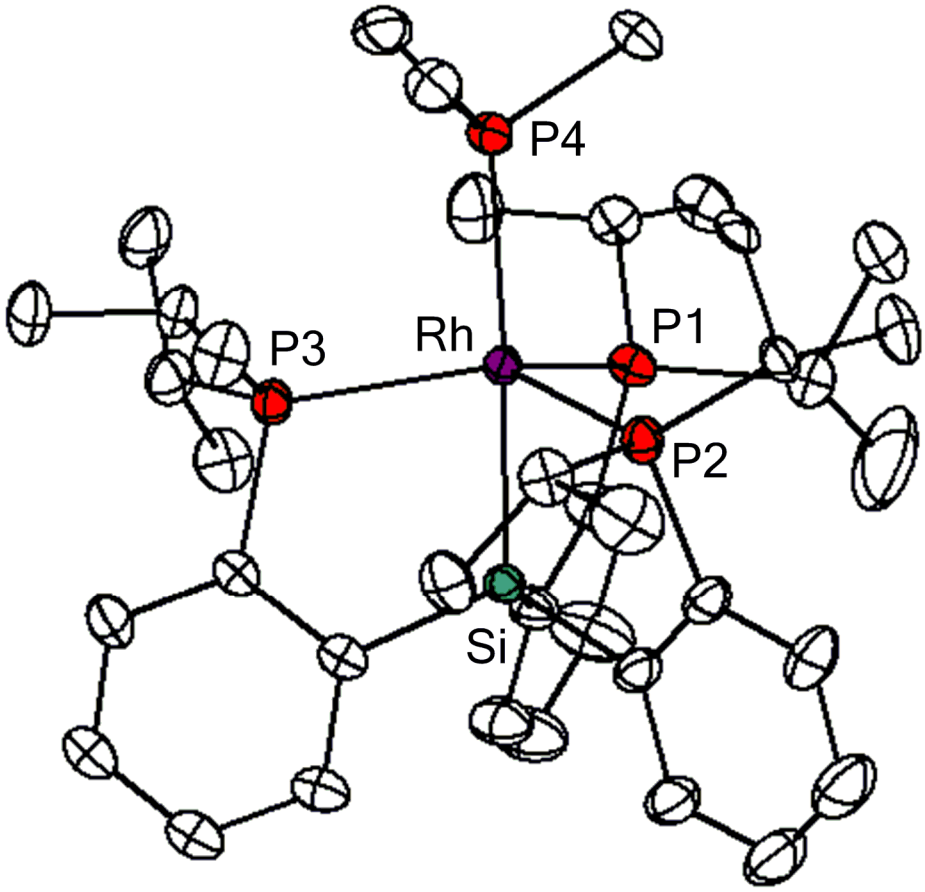

BAr$^{\mathrm{F}}_4$ anion and hydrogen atoms removed for clarity.

Table 3. Crystal data and structure refinement for {**[SiP$^{iPr}_3$]Ir(PMe$_3$)}OTf (3')**

Identification code	09289	
Empirical formula	C40 H53 Cl4 F3 Ir O3 P4 S Si	
Formula weight	1156.85	
Temperature	100(2) K	
Wavelength	0.71073 Å	
Crystal system	Monoclinic	
Space group	P2(1)/c	
Unit cell dimensions	a = 10.7531(11)Å	□= 90°.
	b = 30.421(3) Å	□= 101.115(2)°.
	c = 15.5269(16) Å	□ = 90°.
Volume	4983.9(9) Å^3	
Z	4	
Density (calculated)	1.542 Mg/m^3	
Absorption coefficient	3.133 mm^{-1}	
F(000)	2316	
Crystal size	0.50 x 0.50 x 0.05 mm^3	
Theta range for data collection	2.23 to 28.51°.	
Index ranges	-14<=h<=14, -40<=k<=40, -20<=l<=20	
Reflections collected	101689	
Independent reflections	12377 [R(int) = 0.0637]	
Completeness to theta = 33.13°	100.0 %	
Absorption correction	Semi-empirical from equivalents	
Max. and min. transmission	0.8591 and 0.3034	
Refinement method	Full-matrix least-squares on F^2	
Data / restraints / parameters	12377 / 57 / 575	
Goodness-of-fit on F^2	1.091	
Final R indices [I>2sigma(I)]	R1 = 0.0432, wR2 = 0.0973	
R indices (all data)	R1 = 0.0565, wR2 = 0.1044	
Largest diff. peak and hole	2.441 and -1.733 e.Å^{-3}	

Figure 18. Solid-state Structure of {**[SiP$^{i\mathrm{Pr}}_3$]Ir(PMe$_3$)}OTf (3')**.

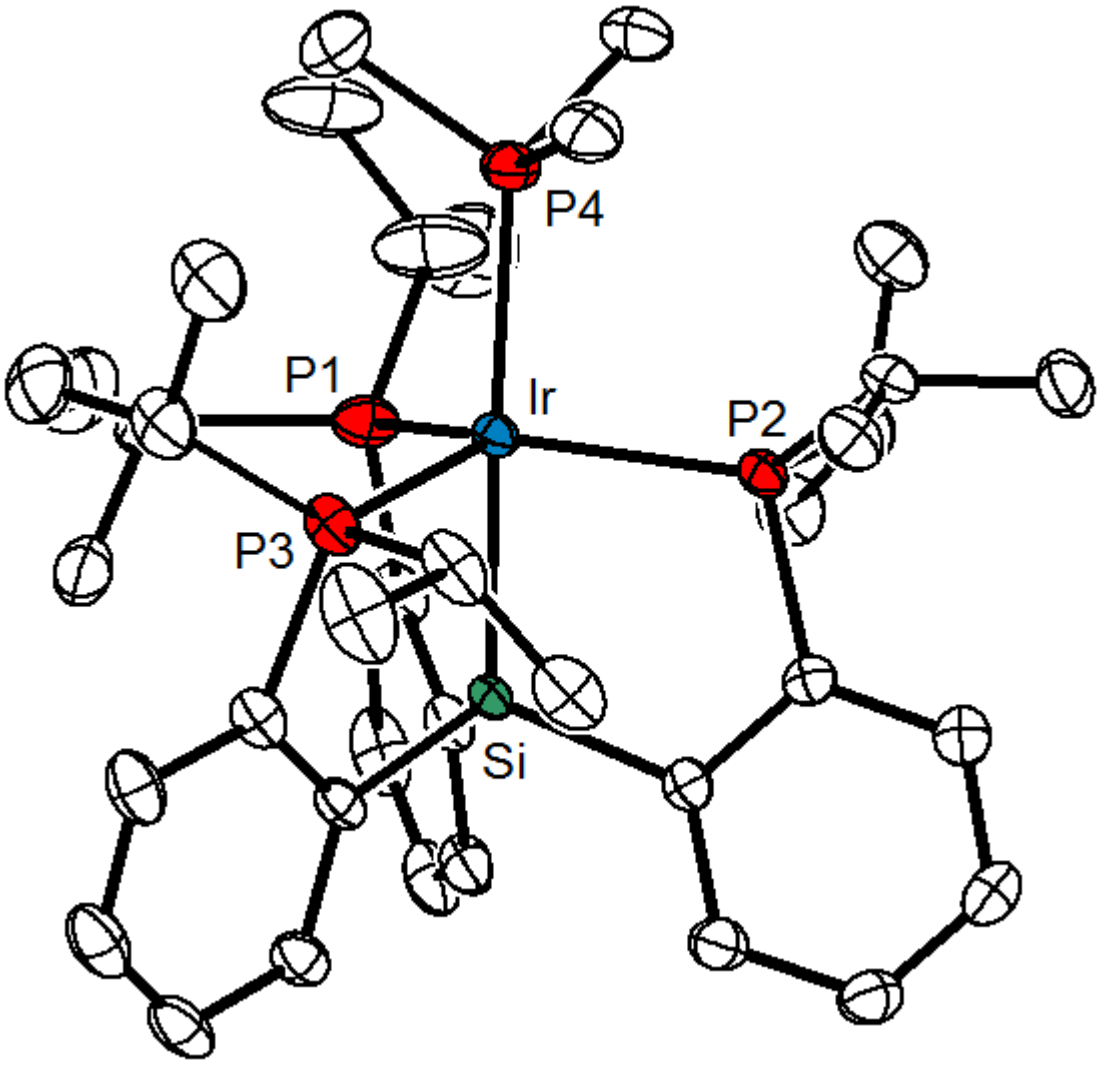

Hydrogen atoms, OTf anion, and solvent molecules removed for clarity.

Table 4. Spin density calculated from optimized structure and x-ray coordinates of **[SiP$^{iPr}_3$]Co(PMe$_3$)}BAr$^F_4$ (1)**.

Opt			Xray		
1	Co	1.177209	1	Co	1.129279
2	P	-0.02313	2	P	-0.02683
3	P	-0.01959	3	P	-0.02087
4	P	0.003141	4	P	0.023967
5	Si	-0.09923	5	Si	-0.08338
6	C	-4.1E-05	6	C	-0.00303
7	C	0.007381	7	C	0.002832
8	H	-0.00108	8	H	-0.00038
9	C	-0.00316	9	C	-0.00474
10	H	-4.6E-05	10	H	0.000372
11	C	-0.00098	11	C	-0.00139
12	C	-0.00032	12	C	-0.0004
13	H	0.000232	13	H	0.000294
14	H	0.000091	14	H	0.000158
15	H	-3E-06	15	H	-9.1E-05
16	C	0.001327	16	C	0.002121
17	H	0.000487	17	H	0.000913
18	C	0.00061	18	C	0.002123
19	H	0.000513	19	H	0.000879
20	H	0.000507	20	H	0.00067
21	H	0.000244	21	H	0.000332
22	C	0.000636	22	C	0.002064
23	C	-0.00153	23	C	-0.00128
24	H	0.000065	24	H	0.000075
25	C	-0.00079	25	C	-0.00065
26	H	0.000022	26	H	0.000029
27	C	0.000201	27	C	0.000337
28	H	-3.1E-05	28	H	0.00005
29	H	0.000012	29	H	0.000026
30	H	0.000027	30	H	0.000043
31	C	-0.00085	31	C	-0.00059
32	H	-1E-06	32	H	0
33	C	-0.00606	33	C	0.001381
34	H	0.000509	34	H	-0.00036
35	C	-5.7E-05	35	C	-0.00213
36	H	-3.1E-05	36	H	0.000545
37	C	-0.00321	37	C	-0.00459
38	C	0.005477	38	C	0.001483
39	C	-0.00112	39	C	-0.00123
40	H	0.000327	40	H	0.000347

41	H	0.00021	41	H	0.000246
42	H	-0.00033	42	H	-0.00024
43	C	0.000634	43	C	0.001305
44	H	0.000041	44	H	0.00013
45	H	-0.00048	45	H	-0.00137
46	H	-6.1E-05	46	H	-0.00013
47	C	0.003006	47	C	0.004172
48	H	0.000036	48	H	0.000131
49	H	-0.00321	49	H	-0.00603
50	H	0.000206	50	H	0.000382
51	C	-7.3E-05	51	C	0.000484
52	H	-1.8E-05	52	H	-4.7E-05
53	H	0.000026	53	H	-4.8E-05
54	H	0.000191	54	H	0.00022
55	C	-0.00308	55	C	-0.00278
56	H	0.000323	56	H	0.000346
57	C	-0.00011	57	C	0.000602
58	H	-3E-06	58	H	0.000004
59	H	-6.7E-05	59	H	-0.00013
60	H	-5.2E-05	60	H	0.000159
61	C	-0.00128	61	C	-0.00288
62	C	0.005784	62	C	0.008499
63	H	0.000422	63	H	0.001238
64	C	0.000671	64	C	0.002272
65	H	0.000524	65	H	0.000733
66	H	-5.1E-05	66	H	-9.3E-05
67	H	-5.1E-05	67	H	-0.00013
68	C	-0.0034	68	C	-0.00242
69	H	-0.00119	69	H	-0.001
70	C	0.000105	70	C	0.000488
71	H	-6.7E-05	71	H	-8.1E-05
72	H	-0.00006	72	H	-0.00086
73	H	0.000024	73	H	0.000074
74	C	0.000162	74	C	0.000149
75	H	-3.7E-05	75	H	-7.9E-05
76	H	0.000123	76	H	0.000062
77	H	-1.6E-05	77	H	-1.6E-05
78	C	0.000214	78	C	0.000442
79	H	-0.00018	79	H	-9.3E-05
80	C	-0.00318	80	C	0.003528
81	H	0.000102	81	H	-0.00058
82	C	-0.00065	82	C	0.000096
83	H	-3.5E-05	83	H	0.000065

84	C	-0.00115	84	C	-0.0009
85	H	-0.00014	85	H	-6.1E-05
86	C	0.000263	86	C	0.00037
87	H	0.000021	87	H	0.000086
88	H	0.000045	88	H	0.00007
89	H	0.000068	89	H	0.000068
90	C	0.000672	90	C	0.001177
91	H	-0.0001	91	H	-0.0002
92	C	0.000644	92	C	0.000219
93	H	-0.00013	93	H	-2.3E-05
94	C	0.000737	94	C	0.000509
95	H	-0.00006	95	H	-0.00012
96	H	-4.5E-05	96	H	-1.8E-05
97	H	0.000311	97	H	0.000225
98	P	-0.02967	98	P	-0.02047
99	C	-0.00418	99	C	-0.00559
100	H	-0.00128	100	H	-0.00106
101	C	0.000341	101	C	0.000487
102	H	0.000034	102	H	-4.5E-05
103	H	0.000048	103	H	0.000132
104	H	0.000259	104	H	0.000043
105	C	0.000321	105	C	0.000189
106	H	0.000036	106	H	-0.00013
107	H	0.000084	107	H	0.000073
108	H	-2.6E-05	108	H	-0.00025

Table 5. Coordinates of optimized structure of **[SiP$^{iPr}_3$]Co(PMe$_3$)}BAr$^F_4$ (1)**.

Co	-0.01476	-0.01464	-0.85087
P	-0.07464	0.119756	-3.22295
P	2.308968	-1.01919	-0.56397
P	-0.21231	2.379104	-0.24294
Si	0.085678	-0.15974	1.453934
C	2.34777	-1.8364	1.09913
C	3.33767	-3.32185	2.778269
H	4.127357	-4.00696	3.076123
C	2.276405	-3.03756	3.660234
H	2.239088	-3.51022	4.638624
C	-1.62997	-0.45402	2.21719
C	-1.38176	1.173896	-4.0143
H	-1.18887	2.231567	-3.80452
H	-2.37877	0.929325	-3.63801
H	-1.37643	1.036883	-5.10338
C	2.590644	-2.39722	-1.83884
H	2.486596	-1.86258	-2.79623
C	-0.31661	-1.47603	-4.14351
H	-0.45077	-1.28283	-5.21586
H	-1.19223	-2.01831	-3.77594
H	0.557961	-2.12208	-4.01999
C	0.769486	1.455177	2.17529
C	1.396172	1.554213	3.440618
H	1.530453	0.66315	4.050515
C	1.737684	3.942189	3.128722
H	2.107687	4.898753	3.489245
C	4.433046	0.409375	-1.92237
H	3.798221	1.232495	-2.26279
H	4.446095	-0.36054	-2.70272
H	5.454491	0.802776	-1.83584
C	-3.96122	-1.17429	1.931747
H	-4.77279	-1.54966	1.315256
C	3.374981	-2.72111	1.50801
H	4.210062	-2.94703	0.853475
C	-2.01481	2.88941	0.096952
H	-2.48024	1.936044	0.381966
C	0.635996	2.626435	1.380764
C	1.296904	-1.51199	2.001001
C	1.400156	0.768704	-4.14308
H	2.298127	0.190548	-3.90558
H	1.590685	1.814301	-3.88274
H	1.226253	0.70891	-5.22544

C	-1.07965	-3.72858	0.708157
H	-1.48407	-3.56552	1.713805
H	-0.11122	-3.23069	0.653878
H	-0.9119	-4.80671	0.586214
C	1.466253	-3.45554	-1.75378
H	1.534919	-4.14535	-2.60564
H	0.470502	-3.0015	-1.76289
H	1.561705	-4.04908	-0.83787
C	3.964249	-3.11714	-1.86927
H	4.068544	-3.81733	-1.03422
H	4.819112	-2.43412	-1.86007
H	4.031206	-3.70956	-2.79206
C	0.476334	3.687617	-1.42789
H	-0.03009	3.430804	-2.37085
C	0.208092	5.198383	-1.17123
H	0.942528	5.624321	-0.48025
H	-0.78853	5.412884	-0.78113
H	0.316007	5.743012	-2.11918
C	-2.67177	-0.95909	1.388171
C	-2.07662	-3.2413	-0.36923
H	-1.66618	-3.48877	-1.36056
C	-3.40608	-4.01916	-0.19096
H	-3.18263	-5.09423	-0.17588
H	-4.12635	-3.85189	-0.99729
H	-3.88518	-3.77618	0.764971
C	3.982741	-0.13549	-0.54668
H	4.693769	-0.92122	-0.25063
C	1.994869	3.47376	-1.63037
H	2.353363	4.081763	-2.472
H	2.232927	2.426787	-1.83203
H	2.554667	3.780078	-0.7393
C	-2.74673	3.407551	-1.16896
H	-3.82813	3.417159	-0.98274
H	-2.56932	2.782119	-2.04891
H	-2.45415	4.43157	-1.41968
C	1.882662	2.784151	3.916799
H	2.371307	2.840917	4.886367
C	1.273549	-2.13149	3.273901
H	0.461797	-1.91599	3.965761
C	-1.92194	-0.16939	3.574349
H	-1.14969	0.24751	4.217633
C	-3.2041	-0.38589	4.108588
H	-3.40774	-0.15556	5.151341

C	4.042607	0.963582	0.539765
H	5.051509	1.396667	0.562563
H	3.828149	0.565056	1.536774
H	3.333844	1.77308	0.342164
C	1.112606	3.864192	1.871856
H	0.999514	4.772823	1.294009
C	-4.22666	-0.89064	3.282687
H	-5.2233	-1.05575	3.684105
C	-2.22984	3.863863	1.281852
H	-1.76056	4.839878	1.113794
H	-1.83802	3.459751	2.220031
H	-3.30752	4.033337	1.413393
P	-2.23173	-1.33729	-0.3703
C	-3.87837	-1.12495	-1.27751
H	-4.59038	-1.75699	-0.73209
C	-3.83346	-1.64501	-2.73465
H	-4.84609	-1.62627	-3.15851
H	-3.46755	-2.67542	-2.80969
H	-3.20598	-1.01256	-3.37011
C	-4.41786	0.319804	-1.23368
H	-3.77098	1.00438	-1.78842
H	-4.51576	0.69499	-0.20898
H	-5.41276	0.354055	-1.69771

Table 6. Coordinates of optimized structure of **[SiP$^{i\mathrm{Pr}}_3$]Rh(PMe$_3$)}BAr$^{\mathrm{F}}_4$ (2)**.

Rh	-0.06802	-0.69268	-0.37791
Si	-0.12276	1.535807	0.370782
P	0.589599	-1.05456	2.001318
P	2.011292	0.217386	-1.50341
P	-2.53088	-0.21603	-0.66855
P	0.002666	-3.06615	-1.3144
C	0.870343	1.71479	1.979387
C	1.285577	2.972009	2.482825
H	1.085841	3.877522	1.913364
C	1.97919	3.078997	3.699799
H	2.293015	4.052899	4.06715
C	2.266897	1.916265	4.43999
H	2.796866	1.986517	5.386477
C	1.877498	0.658329	3.950923
H	2.119562	-0.21967	4.536299
C	1.194183	0.542709	2.715074
C	0.765469	2.657215	-0.87119
C	0.543508	4.049504	-0.99632
H	-0.27711	4.517762	-0.45673
C	1.360512	4.845526	-1.81847
H	1.170781	5.912154	-1.90954
C	2.436113	4.25761	-2.51223
H	3.087456	4.869628	-3.131
C	2.664573	2.873906	-2.41105
H	3.504542	2.447368	-2.94988
C	1.818624	2.060548	-1.61966
C	-1.89694	2.121757	0.722809
C	-2.19392	3.312353	1.429571
H	-1.3877	3.951841	1.782061
C	-3.51905	3.67672	1.726539
H	-3.72324	4.591057	2.277911
C	-4.57868	2.842844	1.322714
H	-5.60589	3.110015	1.557443
C	-4.30727	1.656789	0.618268
H	-5.14278	1.027183	0.326257
C	-2.97581	1.288889	0.313826
C	-0.70712	-1.59057	3.273306
H	-1.18647	-2.47102	2.819124
C	-1.77079	-0.47756	3.442777
H	-2.61821	-0.8644	4.023277
H	-2.15096	-0.1072	2.489249
H	-1.35186	0.37484	3.989531

C	-0.19012	-1.98803	4.681298
H	0.178005	-1.11223	5.226101
H	0.598215	-2.74482	4.668232
H	-1.02847	-2.39818	5.260832
C	1.98581	-2.34458	2.085052
H	2.426027	-2.23896	1.085423
C	1.418753	-3.78496	2.192182
H	2.18146	-4.5056	1.867974
H	0.52871	-3.93412	1.577871
H	1.156791	-4.03943	3.223242
C	3.14059	-2.16639	3.101981
H	2.80627	-2.28849	4.13814
H	3.637769	-1.19679	3.010298
H	3.894439	-2.94347	2.91146
C	2.035522	-0.39371	-3.30224
H	2.017486	-1.48711	-3.18712
C	0.743339	0.028596	-4.04001
H	0.712598	1.1143	-4.18507
H	-0.1558	-0.26748	-3.49069
H	0.710677	-0.44194	-5.03189
C	3.26431	-0.04425	-4.18047
H	3.210156	-0.62884	-5.10912
H	4.222593	-0.2777	-3.70637
H	3.265295	1.011547	-4.46948
C	3.822543	0.065118	-0.98645
H	4.377458	0.65488	-1.73077
C	4.081438	0.711586	0.393529
H	3.528503	0.204518	1.189703
H	3.796328	1.768731	0.41102
H	5.151505	0.648916	0.631406
C	4.360002	-1.3837	-1.03472
H	5.429532	-1.38293	-0.78716
H	4.253983	-1.84477	-2.02352
H	3.856	-2.02555	-0.30399
C	-2.92485	0.360845	-2.44774
H	-2.53428	-0.43662	-3.0992
C	-2.18669	1.67827	-2.79041
H	-2.28686	1.881796	-3.8646
H	-1.12173	1.649396	-2.55303
H	-2.62834	2.521721	-2.24773
C	-4.43159	0.549656	-2.7628
H	-4.87779	1.318036	-2.12067
H	-5.01934	-0.36827	-2.6695

H	-4.53348	0.895676	-3.80013
C	-3.95578	-1.41163	-0.33499
H	-4.87121	-0.82847	-0.50005
C	-3.98877	-1.92233	1.122691
H	-4.8244	-2.62408	1.245732
H	-4.12972	-1.10832	1.840005
H	-3.06578	-2.45262	1.38681
C	-3.99159	-2.5986	-1.32797
H	-3.15219	-3.27853	-1.17048
H	-3.98665	-2.27971	-2.376
H	-4.91202	-3.17496	-1.1666
C	1.636845	-3.9283	-1.52079
H	1.492227	-4.9277	-1.95165
H	2.137236	-4.0373	-0.55396
H	2.298369	-3.36128	-2.18308
C	-0.9566	-4.44416	-0.48464
H	-1.52776	-5.01616	-1.22559
H	-1.64969	-4.05699	0.267117
H	-0.26791	-5.1385	0.007816
C	-0.6311	-3.21944	-3.0559
H	-0.03928	-2.60264	-3.7387
H	-1.67289	-2.88985	-3.11588
H	-0.57615	-4.26173	-3.39639

Table 7. Coordinates of optimized structure of **[SiP$^{i\mathrm{Pr}}_3$]Ir(PMe$_3$)}BAr$^{\mathrm{F}}_4$ (3)**.

Ir	-0.06038	-0.69075	-0.19321
Si	-0.09528	1.675878	-0.02377
P	0.451295	-0.48505	2.183996
P	2.028453	-0.17337	-1.36273
P	-2.42781	-0.3053	-0.67652
P	-0.01866	-3.14244	-0.49375
C	0.784193	2.218869	1.566465
C	1.18172	3.555516	1.811561
H	1.026314	4.315609	1.048388
C	1.79897	3.926093	3.0176
H	2.102145	4.956607	3.184777
C	2.022446	2.951465	4.008789
H	2.491596	3.225012	4.950458
C	1.64567	1.617426	3.781111
H	1.835349	0.892205	4.561603
C	1.042742	1.234493	2.557222
C	0.922321	2.427477	-1.42656
C	0.815709	3.757432	-1.89719
H	0.014292	4.397877	-1.53429
C	1.722002	4.270695	-2.84134
H	1.619988	5.291781	-3.20029
C	2.77304	3.458488	-3.30921
H	3.493478	3.852644	-4.02148
C	2.890073	2.131904	-2.85891
H	3.716099	1.534464	-3.22925
C	1.953852	1.596041	-1.94244
C	-1.87037	2.338772	0.046185
C	-2.20322	3.676613	0.366056
H	-1.41553	4.404099	0.550088
C	-3.54155	4.089414	0.487678
H	-3.77524	5.12023	0.741532
C	-4.57719	3.155711	0.296691
H	-5.61539	3.460604	0.400615
C	-4.26976	1.822188	-0.02646
H	-5.09144	1.125601	-0.16236
C	-2.9243	1.404779	-0.15469
C	-0.94555	-0.67801	3.455276
H	-1.42911	-1.63058	3.192395
C	-1.97796	0.466054	3.307046
H	-2.85612	0.247808	3.928534
H	-2.31501	0.606302	2.279752
H	-1.55261	1.415067	3.652432

C	-0.52092	-0.74183	4.947193
H	-0.16818	0.234417	5.295399
H	0.249917	-1.48491	5.161386
H	-1.40203	-0.99951	5.550457
C	1.796	-1.733	2.700588
H	2.302115	-1.88674	1.740498
C	1.187776	-3.09561	3.129288
H	1.942151	-3.88577	3.015777
H	0.313078	-3.37572	2.541001
H	0.890096	-3.09054	4.181556
C	2.88967	-1.32464	3.719284
H	2.489976	-1.1923	4.730718
H	3.41756	-0.41122	3.433473
H	3.632341	-2.13348	3.769109
C	2.179222	-1.19876	-2.96393
H	2.072932	-2.23191	-2.60532
C	1.008434	-0.90403	-3.93269
H	1.074829	0.116734	-4.32584
H	0.032191	-1.01909	-3.45436
H	1.055252	-1.59341	-4.7866
C	3.510558	-1.13946	-3.76132
H	3.503079	-1.94739	-4.50568
H	4.403971	-1.27657	-3.14562
H	3.609542	-0.20085	-4.31537
C	3.799214	-0.21713	-0.69147
H	4.398658	0.174152	-1.52608
C	4.000449	0.750053	0.496324
H	3.429895	0.439627	1.3753
H	3.702918	1.774158	0.249043
H	5.06285	0.766983	0.773878
C	4.33316	-1.62863	-0.35447
H	5.395474	-1.55657	-0.08616
H	4.255593	-2.32805	-1.19417
H	3.812168	-2.06835	0.502008
C	-2.69718	-0.19441	-2.56884
H	-2.28666	-1.13582	-2.96444
C	-1.91342	0.986351	-3.19269
H	-1.95169	0.906838	-4.28716
H	-0.86466	1.01166	-2.89476
H	-2.36734	1.943308	-2.91203
C	-4.17743	-0.07276	-3.01744
H	-4.63723	0.838686	-2.61798
H	-4.79926	-0.92838	-2.74033

H	-4.20415	0.005509	-4.11251
C	-3.90726	-1.37197	-0.16694
H	-4.78194	-0.8161	-0.52783
C	-4.06372	-1.52899	1.361593
H	-4.93946	-2.15598	1.575443
H	-4.21276	-0.56701	1.859925
H	-3.19004	-2.01391	1.812757
C	-3.9445	-2.75366	-0.86268
H	-3.15895	-3.41326	-0.49356
H	-3.85569	-2.68671	-1.95176
H	-4.90487	-3.23867	-0.64345
C	1.587307	-4.06878	-0.38827
H	1.417426	-5.13651	-0.57865
H	2.031099	-3.96091	0.605495
H	2.306413	-3.69884	-1.12354
C	-1.05981	-4.24559	0.604141
H	-1.66724	-4.9254	-0.00384
H	-1.72359	-3.65998	1.244629
H	-0.41706	-4.86302	1.23966
C	-0.57658	-3.72124	-2.17025
H	0.070473	-3.3201	-2.9553
H	-1.60031	-3.39311	-2.37304
H	-0.54652	-4.8174	-2.22434

Figure 19. UV-VIS spectrum of [SiP$^{iPr}_3$]Rh(N_2) (5) under N_2 and after several freeze-pump-thaw cycles.

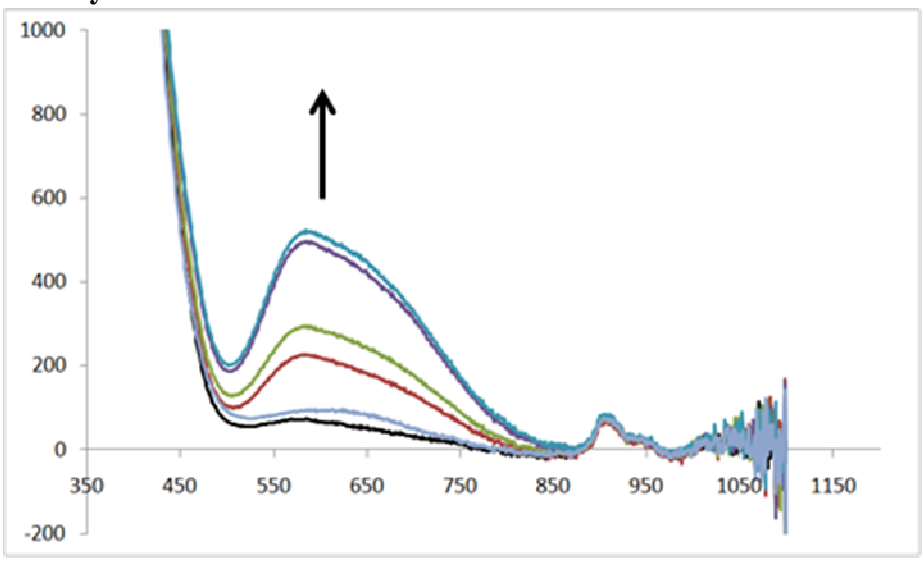

Y-axis: molar absorptivity. X-axis: wavelength (nm)

Arrow shows the growing of peak at 592 nm after several freeze-pump-thaw cycles corresponding to loss of N_2 (in THF).

Figure 20. Relative energies of the frontier orbitals for complexes 1-3 and their molecular orbitals (energies in Hartrees).

	Co complex, **1**	Rh complex, **2**	Ir complex, **3**
LUMO	-0.14723	-0.13057	-0.12631
SOMO	-0.30776	-0.28441	-0.27665
SOMO-1	-0.31681	-0.30493	-0.30361
E(SOMO)-E(SOMO-1)	0.00905	0.02052	0.02696

Orbitals of Co complex, 1 (LUMO, SOMO, SOMO-1 from left to right)

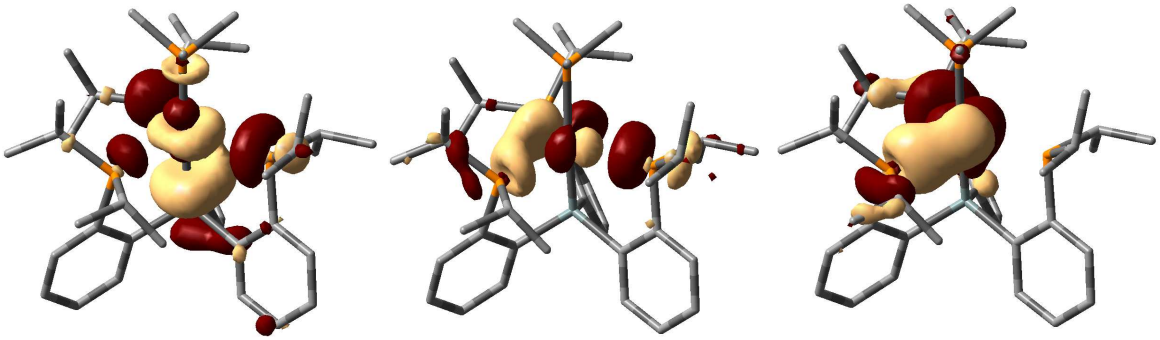

Orbitals of Rh complex, 2 (LUMO, SOMO, SOMO-1 from left to right)

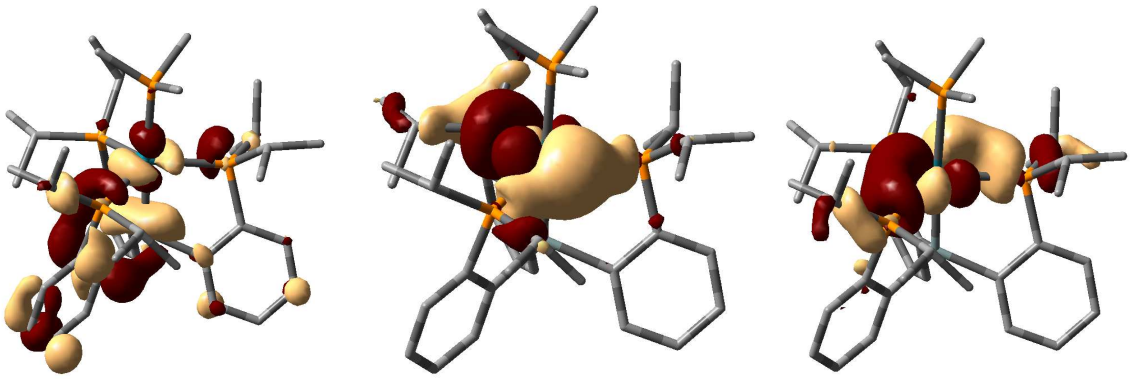

Orbitals of Ir complex, 3 (LUMO, SOMO, SOMO-1 from left to right)